



# 1      **Characterization of chromophoric dissolved organic matter in** 2      **lakes on the Tibet Plateau, China, using spectroscopic analysis**

3              Kaishan Song<sup>1##</sup>, Sijia Li<sup>2#</sup>, Zhidan Wen<sup>1</sup>, Lili Lyu<sup>1</sup>, Yingxin Shang<sup>1</sup>

4              <sup>1</sup> Northeast Institute of Geography and Agroecology, CAS, Changchun, 130102, China

5              <sup>2</sup> School of Environmental, Northeast Normal University, Changchun, 136000, China

6      # first co-authors

7      \*authors correspondence should be addressed: songkaishan@neigae.ac.cn

8      **Abstract** Spatiotemporal variations in the characteristics of fluorescent dissolved  
 9      organic matter (FDOM) components from 63 lakes across the Tibet Plateau, China, are  
 10      examined using excitation-emission matrix spectra (EEM) and fluorescence regional  
 11      integration (FRI) from 2014 to 2017. Freshwater ( $N=135$ ) and brackish water ( $N=109$ )  
 12      samples from 63 lakes were grouped according to salinity or electrical conductivity. In  
 13      order to compare results between the lakes, cumulative volumes beneath the EEM  
 14      values ( $\phi_i$ ,  $i=I, II, III, IV, V$ ) were normalized to a DOC concentration of 1 mg/L. EEM-  
 15      FRI identified tyrosine-like ( $\phi_I$ ), tryptophan-like ( $\phi_{II}$ ), fulvic-like ( $\phi_{III}$ ), microbial  
 16      protein-like ( $\phi_{IV}$ ), and humic-like ( $\phi_V$ ) fluorescence regions, as well as their proportions  
 17      ( $P_i$ ). Chromophoric dissolved organic matter (CDOM) absorption parameters,  
 18      fluorescence indices, average fluorescence intensities of the five fluorescent  
 19      components and total fluorescence intensities ( $\phi_T$ ) differed under spatial variation  
 20      among brackish and freshwater lakes (ANOVA,  $p<0.05$ ). Principal component analysis  
 21      (PCA) was used to assess and group five normalized FDOM components for all of the  
 22      water samples. These results show that microbial protein-like ( $\phi_{IV}$ ), fulvic-like ( $\phi_{III}$ )  
 23      and humic-like ( $\phi_V$ ) have positive correlations ( $R^2>0.79$ ,  $t$ -test,  $p<0.01$ ), indicating that  
 24      these FDOM components may originate from similar sources. A correlation also exists





25 between normalized  $\phi_i$  ( $i=I, II, III, IV, V$ ) and DOC concentrations with a salinity  $>19\text{‰}$   
26 (averaged EC,  $23764\mu\text{s cm}^{-1}$ ) ( $t$ -test,  $p<0.01$ ), of which  $R^2$  regression analysis showed  
27 a decreasing tendency with EC. Similar correlations between  $a(254)$  and DOC  
28 concentrations ( $t$ -test,  $p<0.01$ ) are also evident for sunshine hours  $> 2900$  h.  
29 Redundancy analysis (RDA) indicates that  $a(254)$  and  $a(350)$  have a correlation with  
30 CDOM in brackish lakes.  $a(254)$ ,  $HIX$  and  $a(350)$  were also correlated with water  
31 quality. Strong evapoconcentration, intense ultraviolet irradiance and landscape  
32 features of the Tibet Plateau may be responsible for the FDOM characteristics identified  
33 in this study.

34 Keywords: CDOM; Tibet Plateau; Fluorescence; Brackish lakes; FRI



35

## 36 1. Introduction

37 ~~Inland lakes are a direct link between the land and atmospheric CO<sub>2</sub> pools and rivers,~~  
38 ~~and they are an indirect link between the oceans (via rivers).~~ Inland lakes play an  
39 important role in the transport  transformation and storage of carbon from  
40 terrestrially imported substances (Cole et al., 2007; Tranvik et al., 2009). Carbon flux  
41 and biogeochemical processes of lakes have a significant influence on the global carbon  
42 cycle, on the aquatic ecosystem, and they confer regional effects on climate (Battin et  
43 al., 2009; Jiao et al., 2010; Ran et al., 2013; Carlson et al., 2011). However,  
44 anthropogenic activities (i.e., industrial, agricultural and domestic sewage) can alter the  
45 carbon balance and interfere with biogeochemical cycling of lakes, ~~effects~~ which can  
46 be recorded in spatiotemporal variations of dissolved carbon within the catchment. It is  
47 therefore important to investigate biogeochemical  cycling of carbon in lakes in different  
48 regions that have distinct properties (Cole et al., 2007; Falkowski et al., 2000).

49 The Tibet Plateau, commonly known as the ‘Third Pole’ or the ‘Asian water tower’,  
50 possesses an average elevation over 4500 m, and contains the largest ice mass outside  
51 the polar regions (Song et al., 2016). This region also contains the greatest number of  
52 large-scale lakes and glaciers in the world. The total area of lakes on the Tibet Plateau  
53 account for about 49% of the total lake area in China (Zhang et al., 2011). As of 2011,  
54 there were 312, 104, 7 and 3 lakes with surface areas greater than 10 km<sup>2</sup>, 100 km<sup>2</sup>, 500  
55 km<sup>2</sup> and 1000 km<sup>2</sup>, respectively (Zhang et al., 2011). In addition, due to dry and thin  
56 air with a low concentration of ozone in this area, there are strong Ultraviolet-B (UV-  
57 B) radiation-penetration inhibiting properties (Ren et al., 1997). Prolonged sunshine  
58 and the arid environment ~~has~~ resulted in a high number of lakes in this region having a  
59 high salt content, or having a significant accumulation of dissolved organic carbon



(DOC). DOC and dissolved organic matter (DOM) contents contained in brackish or saline lakes, particularly in arid and semi-arid regions, contribute to the relatively high average DOC concentrations and carbon budget of inland waters (Song et al., 2013; Tranvik et al., 2009; Wen et al., 2016). Due to its high altitude, arid environment, low population density, urbanization, and economic development, the Tibet Plateau is therefore of particular interest for climate change, environmental evolution and the carbon cycle. There is also significant interest to investigate total DOM in brackish and saline lakes across the Tibet Plateau.

DOM (typically  $<0.45 \mu\text{m}$ ) represents one of the largest pools of organic carbon on Earth (Hedges et al., 1992; McKnight et al., 2001). Chromophoric DOM (CDOM, typically  $<0.22 \mu\text{m}$ ), light-absorbing DOM in aquatic environments, originates from the decomposition of algal by microorganisms (autochthonous), as well as through the transport of the surrounding allochthonous environment (Singh et al., 2010; Zhang et al., 2010). Chemical properties cause CDOM to absorb energy and re-emit it as fluorescence (FDOM) (Helms et al., 2008; Stedmon et al., 2003; Zhang et al., 2010). Due to the high selectivity and sensitivity of FDOM, absorption and fluorescence spectroscopy has provided detailed insights into its composition and components (Stedmon et al., 2003; Zhang et al., 2010). ~~Multivariate statistical parameters and tools, i.e., spectroscopic~~ characterization (specific ultraviolet absorbance and spectral slope ratio), excitation-emission matrix (EEM), humification index (*HIX*), fluorescence index (*FI*), parallel factor analysis (PARAFAC) and fluorescence regional integration (FRI), have been utilized to identify bio-geochemically meaningful components of CDOM (Coble, 1996; Helms et al., 2008; Stedmon et al., 2003). EEM-PARAFAC and EEM-FRI techniques can show dynamic and detailed components of FDOM for each EEM, ~~techniques which~~ have been widely used in aquatic environmental dynamics (source



85 and fate) (Chen et al., 2003; Zhang et al., 2010; Zhao et al., 2017). Compared to other  
86 fluorescence tools, EEM-FRI (a quantitative technique) can integrate the volumes  
87 beneath defined by regions of EEM largely based on supporting literature (Chen et al.,  
88 2003). This is related to all of the wavelength ranges of different fluorescence peaks in  
89 each EEM, and covers continuous fluorescence intensity at excitation-emission  
90 wavelength of divided regions for further analysis (Chen et al., 2003).

91 It is believed that the high altitude and arid environment of the Tibet Plateau could  
92 have an influence on CDOM in brackish and saline lakes. These influences may affect  
93 DOC accumulation, result in a high photochemical degradation rate due to prolonged  
94 sunshine, decrease anthropogenic CDOM inputs, and result in an accumulation of  
95 nutrients in lake catchment areas (Spencer et al. 2012; Yao et al., 2011; Song et al.,  
96 2017). Although CDOM optical characteristics and their effect on carbon budget  
97 contribution have been reported in plateaus and high-mountain lakes (Wen et al., 2016;  
98 Zhang et al., 2010), little is currently known about CDOM in the Tibet Plateau. Analysis  
99 in this area could reveal a natural state of composition, sources, dynamics, and fate of  
100 CDOM by comparing results with other brackish and saline lakes with high  
101 eutrophication rates due to increased terrestrial nutrient input. Based on previous  
102 studies, our investigation examines sources and fate of CDOM in brackish (31 lakes)  
103 and saline lakes (32 lakes) across the Tibet Plateau using EEM-FRI. The study  
104 objectives are to: (1) characterize the similarities and differences in CDOM absorption  
105 and components among the 63 lakes with similar climatic, hydrologic and geological  
106 conditions using EEM-FRI technology; (2) investigate and evaluate spatial dynamic  
107 of each fluorescence component using EEM-FRI; (3) link FDOM by EEM-FRI to  
108 CDOM absorption and fluorescence parameters, and to water quality; and (4) assess the  
109 effects on FDOM by EEM-FRI caused by salinity, solar radiation and land cover



## 110 2. Materials and Methods

### 111 2.1 Overview of the Tibet lake

112 As the largest and most extensive plateau in the world, the Tibet Plateau covers an area  
113 in China of about 2.5 million km<sup>2</sup>, having an average elevation of more than 4500 m  
114 above sea level (Zhang et al., 2011). Lakes on the Tibeta Plateau are typically formed  
115 due to erosion and melting of glaciers, geological tectonic activity (fault and  
116 depression), barriers present on the land-surface, or due to melting on hot spots etc. The  
117 majority of these lakes are sensitive to global climate change (Liu and Chen, 2000; Qin  
118 et al., 2009). Due to the diverse climate (some airflows of tropospheric tropical easterly,  
119 subtropical westerly, and southwestern monsoon from the Indian Ocean) and complex  
120 topography (numerous different broad basins or valleys with high mountain ranges) in  
121 this area, annual precipitation ranges from 100 to 1300 mm. The majority of  
122 precipitation occurs during the summer period (June to September). Solar UV radiation  
123 in this area is strong due to dry and thin air, having a low ozone concentration (Ren et  
124 al., 1997). In the winter the climate is dominated by cold and dry westerly winds which  
125 are more pronounced with elevation. During the winter, the northwestern area of the  
126 plateau (where average elevation exceeds 5000 m) is the coldest, having average  
127 temperatures around -40 °C (Song et al., 2016). Owing to diverse climatic patterns,  
128 topographical patterns and few anthropogenic activities, the carbon cycle, climate  
129 change and environment evolution over the Tibet Plateau has seen an increase in interest  
130 recently (Zhao et al., 2017; Song et al., 2017).

131 [Insert Figure 1 about here]

### 132 2.2 Field sampling

133 A total of 244 water samples were collected from 63 lakes across the Tibet Plateau from



134 2014 to 2017. Sample locations for each lake were recorded using a GPS receiver (Table  
135 S1 and Fig. 1). Water samples were collected from lake surfaces (0-50 cm) in 1 L acid-  
136 cleaned plastic bottles. The collected water samples were filtered through a pre-  
137 combusted Whatman GF/F filter (0.7  $\mu\text{m}$ ) and then further filtered through a pre-rinsed  
138 25 mm Millipore membrane cellulose filter (0.22  $\mu\text{m}$ ) into brown plastic bottles.  
139 Samples were prepared for DOC analysis by being filtered through a pre-combusted  
140 Whatman GF/F filter (0.45  $\mu\text{m}$ ) under a low vacuum. The filtered samples were stored  
141 at 4°C and transported to the laboratory for CDOM absorption and fluorescence  
142 analysis within 2 days.

### 143 2.3 Water quality measurements

144 Electrical conductivity (EC) and pH were measured using a portable multi-parameter  
145 water quality analyzer (YSI EXO1, US). DOC concentrations were determined by high-  
146 temperature catalytic oxidation (680 °C) using a total organic carbon analyzer (TOC-  
147 VCPN, Shimadzu, Japan). Potassium hydrogen phthalate was used in this analysis as a  
148 reference. Chlorophyll a (Chl-a) ~~analysis was undertaken~~ by initially filtering the water  
149 samples through Whatman cellulose acetone filters (0.45 $\mu\text{m}$ ) before being extracted  
150 with 90% acetone and measured at 664, 647, 630 and 750 nm wavelengths using a  
151 Shimadzu UV-2006 PC spectrophotometer. Total nitrogen (TN) and Total phosphorus  
152 (TP) were measured following methods highlighted in standard methods  
153 (APHA/AWWA/WEF, 1998).

### 154 2.4 CDOM absorption measurements

155 Absorption spectra of filtered samples were measured between 200 and 800 nm at 1 nm  
156 increments using a Shimadzu UV-2006 PC spectrophotometer with a 1 cm (or 5 cm)  
157 quartz cuvette and Milli-Q water as a reference. The absorption coefficient  $a_{\text{CDOM}}$  was



158 calculated from the measured sample optical absorption  $a(\lambda)$ :

$$159 \quad a_{\text{CDOM}}(\lambda) = 2.303 \text{OD}(\lambda) / \gamma \quad (1)$$

160 where,  $\text{OD}(\lambda)$  is the corrected optical density at wavelength  $\lambda$ ;  $\gamma$  is the cuvette path  
 161 length (0.01 or 0.05 m); and the factor of 2.303 converts the results from a base 10 to a  
 162 base natural logarithm (Zhang et al., 2011). The  $\text{SUVA}_{254}$ ,  $S_{275-295}$  and  $M(E_{250}:E_{365})$   
 163 were used to characterize CDOM features (Helms et al., 2008).

## 164 2.5 Excitation-emission matrix (EEM) fluorescence

165 Three-dimensional excitation-emission matrix (EEM) spectra of CDOM were  
 166 measured at room temperature ( $20 \pm 2$  °C) using a Hitachi F-7000 fluorescence  
 167 spectrometer with a 700 volt xenon lamp. Scanning band pass widths of excitation and  
 168 emission spectra were obtained using wavelengths of 220-450 nm (with intervals of 5  
 169 nm) and 250-600 nm (1 nm intervals), respectively, with a scanning speed of 2400  
 170  $\text{nm} \cdot \text{min}^{-1}$ . A Milli-Q water blank was analyzed, the result of which was subtracted from  
 171 the resulting EEM of the water sample spectrum to eliminate Raman scatter peaks. In  
 172 order to eliminate the inner filter effect, the EEMs were normalized by subtracting the  
 173 integral area under the curve of the Milli-Q water Raman peak according to the methods  
 174 recommended by Zhang et al. (2010) and Zhou et al. (2016). These EEM spectra were  
 175 then calibrated in quinine sulfate units (QSU) (Lawaetz and Stedmon, 2009).

176 The fluorescence indices  $FI_{370}$  and  $FI_{310}$ , defined as  $\text{Ex/Em} = (370/450$   
 177  $\text{nm}) / (370/500 \text{ nm})$  and  $\text{Ex/Em} = (310/380 \text{ nm}) / (310/430 \text{ nm})$ , introduced by McKnight  
 178 et al. (2001), were used to characterize CDOM source.  $FI_{370}$  is used to distinguish fulvic  
 179 acids derived from terrestrial ( $FI_{370} < 1.4$ ) and microbial ( $FI_{370} > 1.9$ ) sources, and  $FI_{310}$   
 180 is used to distinguish autochthonous ( $FI_{310} < 0.7$ ), autochthonous biological activity  
 181 ( $FI_{310} > 0.8$ ) and intermediate autochthonous ( $0.7 < FI_{310} < 0.8$ ) (Zhang et al., 2010). The  
 182 humification index (HIX) is calculated from fluorescence EEMs, as indices for the



183 humification degree and DOM sources (Huguet et al., 2009). Further details of these  
 184 methods are provided in Zhang et al. (2010).

## 185 2.6 EEM fluorescence regional integration

186 EEM Fluorescence Regional Integration (EEM-FRI) divides EEM boundaries into five  
 187 regions associated with humic-like, tyrosine-like, tryptophan-like or phenol-like  
 188 organic compounds, based on the findings of Chen et al. (2003). Fluorescence peaks at  
 189  $Ex < 250$  nm and  $Em < 350$  nm, defined as Regions I and II, relate to aromatic proteins such  
 190 as tyrosine. Peaks at shorter  $Ex < 250$  nm and longer  $Em > 350$  nm are fulvic acid-like  
 191 materials, deemed as Region III. Peaks at intermediate  $250$  nm  $< Ex < 280$  nm and  
 192  $Em < 380$  nm are microbial protein-like, defined as Region IV. Peaks at longer  $Ex > 280$   
 193 nm and  $Em > 380$  nm are related to humic acid-like organics, denoted as Region V. The  
 194 integrated area beneath the EEM spectra can be calculated using:

$$195 \quad \varphi_i = \int_{\lambda_{ex}} \int_{\lambda_{em}} I(\lambda_{ex}, \lambda_{em}) \Delta \lambda_{ex} \Delta \lambda_{em} \quad (2)$$

196 where,  $\Delta \lambda_{ex}$  is  $Ex$  (interval 5 nm);  $\Delta \lambda_{em}$  is  $Em$  (interval 1 nm);  $I(\lambda_{ex}, \lambda_{em})$  is fluorescence  
 197 intensity at each EEM pair; and  $i$  represents the regions of EEM divided by EEM-FRI.  
 198 The cumulative volume in the five regions beneath the EEM can be calculated using  $\varphi_T$   
 199 ( $i = I, II, III, IV, V$ ; unit: nm):

$$200 \quad \varphi_{T,n} = \sum_{i=1}^5 \varphi_{i,n} \quad (3)$$

201 where,  $n$  represents the numbers of cumulative regions in the five regions. The  
 202 cumulative volume beneath the EEM ( $\varphi_i$  and  $\varphi_T$ ) values were normalized to per unit of  
 203 DOC concentration (in mg/L) for comparison of EEMs from different sources. The unit  
 204 of DOC-normalized EEM-FRI is  $QSU \cdot nm^2 \cdot [mg/LC]^{-1}$ . The percent fluorescence  
 205 response in a specific region ( $P_{i,n}$ ,  $i = I, II, III, IV, V$ ) was calculated as:

$$206 \quad P_{i,n} = \frac{\varphi_{i,n}}{\varphi_{T,n}} \times 100\% \quad (4)$$



## 207 2.7 Statistical analysis

208 Statistical analyses, regression and correlation analyses were performed using SPSS  
 209 16.0 (Statistical Program for Social Sciences) to examine the relationships between  
 210 variations (CDOM absorption and fluorescence parameters) among lakes. Significance  
 211 levels are reported as non-significant (NS) ( $p > 0.05$ ), significant (\*,  $0.05 > p > 0.01$ ) or  
 212 highly significant (\*\*,  $p < 0.01$ ). Redundancy analysis (RDA) and principal components  
 213 analysis (PCA) was undertaken using CANOCO 4.5 from two principal components  
 214 analyses (Microcomputer Power, Ithaca, NY, USA).

## 215 3. Results

### 216 3.1 Biogeochemical characteristics

217 Water quality parameters (TN, TP, Chl-a, TSM, pH, EC, turbidity and salinity) for the  
 218 63 lakes (244 water samples) are shown in Table 1. Thirty one lakes were classified as  
 219 brackish ( $N=109$ ;  $35\% > \text{salinity} > 1\%$ ) and 32 lakes were classified as freshwater  
 220 ( $N=135$ ; salinity  $< 1\%$ ). The average values of all water quality parameters in each lake  
 221 were calculated and selected to represent overall water quality of the lake.  
 222 Concentrations of TN (average,  $2.31 \pm 2.64 \text{ mg L}^{-1}$ ), TP (average,  $0.04 \pm 0.03 \text{ mg L}^{-1}$ )  
 223 and Chl-a (average,  $1.45 \pm 2.65 \text{ } \mu\text{g L}^{-1}$ ) were relatively low in fresh lakes ( $N=135$ ),  
 224 coinciding with low turbidity. Brackish lakes, having a eutrophic state, recorded high  
 225 Chl-a (average,  $2.57 \pm 5.73 \text{ } \mu\text{g L}^{-1}$ ), TN (average,  $4.54 \pm 4.32 \text{ mg L}^{-1}$ ) and TP (average,  
 226  $0.45 \pm 1.35 \text{ mg L}^{-1}$ ), results related to their high salt (average,  $6.01 \pm 5.59 \%$ ) and EC  
 227 (average,  $8880.24 \pm 8235.9 \text{ } \mu\text{S cm}^{-1}$ ) contents. The water quality parameters of the  
 228 trophic states slightly higher than the average values for brackish lakes in  
 229 northeastern China (average, TP= $0.11 \text{ mg L}^{-1}$  and TN= $4.07 \text{ mg L}^{-1}$ ; ) in Northeast of  
 230 China (Zhao et al., 2017), and lakes (average, TP= $0.033 \text{ mg L}^{-1}$  and TN= $0.59 \text{ mg L}^{-1}$ ; )



231 in Yungui Plateau of China (Zhang et al., 2010), and lower than those in Hulun Lake  
232 (average, TP=1.52 mg L<sup>-1</sup> and TN=4.58 mg L<sup>-1</sup>; Wen et al., 2016). Zhang et al. (2010)  
233 found that, with an increase in altitude (> 4000 m), oligotrophic lakes increased due to  
234 the natural changes in catchment properties and low human activities. However, for  
235 terminal lakes with less anthropogenic density, there is an accumulation of nutrients  
236 generally derived from allochthonous substances.

237 [Insert Table 1 about here]

238 High concentrations of DOC in brackish waters were found to accumulate in  
239 lakes with high salinity concentrations (Fig. 2a). DOC values for the brackish lakes  
240 were also found to be variable, ranging from 0.27 mg L<sup>-1</sup> in Lake XRC 4.8 mg L<sup>-1</sup>  
241 in Lake CCL with a mean DOC of 35.69 (± 43.52) mg L<sup>-1</sup> (Fig. S1). Mean DOC  
242 concentrations in the fresh lakes were 7.94 ± 12.05 mg L<sup>-1</sup>, recording lower values than  
243 those in brackish lakes. These results are in agreement with the findings of Song et al.  
244 (2013), Zhao et al., (2016) and Wen et al (2016) for brackish lakes in arid and semi-arid  
245 regions. Although brackish lakes have high spatial heterogeneity, results indicate  
246 that decreasing salinity generally coincides with DOC concentrations (Fig. 2b). In  
247 addition, owing to UV-B radiation-penetration inhibiting properties in the Tibet Plateau  
248 (Ren et al., 1997), the tendency linear equation of average DOC concentration showed  
249 a decreased trend with increasing elevation (Fig. 2a). However, variations in DOC  
250 concentrations can also be explained by DOC flux related to physical/chemical  
251 properties, hydrology, and land use/land cover within a specific drainage watershed for  
252 each lake (Heinz et al., 2015; Wen et al., 2016).

253 [Insert Figure 2 about here]

### 254 3.2 CDOM absorption

255 Previous studies have indicated that high salinity could have a direct or indirect impact



on water quality, and they highlighted different structures and composition of DOM (Waiser and Robarts, 2000; Song et al., 2013; Zhang et al., 2010). Generally, Helms et al. (2008) and Weishaar et al. (2003) showed that the absorption coefficient  $a(350)$  is seen as a proxy to characterize CDOM concentration.  $a(350)$  absorption coefficients in our study ranged from 0.09–8.45  $\text{m}^{-1}$  and 0–13.49  $\text{m}^{-1}$  for brackish and fresh lakes, with mean values of 2.38 ( $\pm 3.14$  SD)  $\text{m}^{-1}$  and 1.74 ( $\pm 1.99$  SD)  $\text{m}^{-1}$ , respectively (Fig. 3). These values were found to be significantly different from each other (ANOVA,  $p < 0.05$ ).  $a(254)$  represents the optical properties of DOC aromaticity, and  $\text{SUVA}_{254}$  (the ratio of  $a(254)$  and DOC) can be used to characterize the optical properties of DOC aromaticity (Helms et al., 2008; Spencer et al., 2012). Higher  $\text{SUVA}_{254}$  values are related to allochthonous-dominated sources, having a higher percentage of DOC aromaticity and microbial-dominated substances in DOC; lower  $\text{SUVA}_{254}$  values indicate the opposite (Spencer et al., 2012; Weishaar et al., 2003). Mean  $\text{SUVA}_{254}$  values ranged from 1.47 ( $\pm 2.55$  SD)  $\text{mg C}^{-1} \text{m}^{-1}$  in brackish lakes to 2.29 ( $\pm 1.36$  SD)  $\text{mg C}^{-1} \text{m}^{-1}$  in fresh lakes (Fig. 2). ANOVA analysis indicated there are significant differences ( $p < 0.05$ ) between  $\text{SUVA}_{254}$  values for brackish and fresh lakes.  $\text{SUVA}_{254}$  values for brackish lakes recorded lower values than those recorded in terminal water on the Inner Mongolia Plateau (Brackish,  $\text{SUVA}_{254} = 1.90 \pm 0.57 \text{ mg C}^{-1} \text{m}^{-1}$ ; Fresh,  $\text{SUVA}_{254} = 2.74 \pm 1.08 \text{ mg C}^{-1} \text{m}^{-1}$ ) or in brackish lakes of northeastern China (2.8–5.7  $\text{mg C}^{-1} \text{m}^{-1}$ ) (Zhao et al., 2016; Wen et al., 2016). In this study, the lower  $\text{SUVA}_{254}$  values in the brackish lakes indicated that aromatic moieties of CDOM in this environment were lower than those in fresh lakes, or other brackish environments in China. These differences are due to the effect of photo-degradation and microbial degradation, with prolonged water residence times.

For brackish water lakes,  $M(E_{250}:E_{365})$  ranged from 6.82 in Dajiacuo Lake (DJC)



281 to 74.7 in Gemangcuo Lake (GMC), having an average value of  $28.3 \pm 20.3$  (Fig. 3)  
282 across all brackish lakes. Results for M ( $E_{250}:E_{365}$ ) in fresh lakes ranged from 5.7 in  
283 Tongzecu Lake (TZC) to 89.5 in Lang'angcuo Lake (LAC), having an average value  
284 of  $16.27 \pm 20.6$ . This suggests a significant difference (ANOVA,  $p < 0.05$ ) between fresh  
285 and brackish waters in M ( $E_{250}:E_{365}$ ). The spectral  $S_{275-295}$  (275–295 nm) was used to  
286 represent DOM molecular weight, with higher values signifying lower average  
287 molecular weights of DOC (Helms et al., 2008). Then  $S_{275-295}$  can be regarded as an  
288 indicator for terrestrial DOC percentage (Gonnelli et al., 2013). As shown in Figure 3,  
289 the higher  $S_{275-295}$  values ( $0.0380 \pm 0.009 \text{ nm}^{-1}$ ) in brackish lakes than those in presented  
290 in fresh lakes ( $0.0324 \pm 0.01 \text{ nm}^{-1}$ ; Fig. 3), indicating lower average molecular weight  
291 of DOM. This result showed a significant difference between fresh and brackish lakes  
292 (ANOVA,  $p < 0.05$ ). This implies that chromophores associated with high molecular  
293 weight were destroyed by chemical bond rupture low molecular weight pool in the  
294 photolysis process with a prolonged hydraulic retention time and irradiation (McKnight  
295 et al., 2001). The difference in CDOM absorptio parameters is probably associated to  
296 spatial variations influencing terrestrial inputs from soil and microbial activities due to  
297 plant decay.

298 [Insert Figure 3 about here]

### 299 3.3 EEM-FRI component

300 EEM spectra of CDOM referred to the major fluorescent components and location  
301 information identified using the peak-picking method of Coble (1996) and PARAFAC  
302 from previous studies (Stedmon et al. 2003; Kowalczyk et al., 2010). Typical EEM  
303 spectra of CDOM for four water samples ined from brackish and fresh lakes in the  
304 Tibet Plateau are shown in Figure 4 (a-d). Traditional EEM fluorescence peaks, i.e.,  
305 phytoplankton production ('N' peak), tyrosine-like ('B' peak), humic-like ('M' peak)



306 and tryptophan-like ('T' peak) were observed in the 244 EEM spectra (Coble, 1996).

307 According to Chen et al. (2003), EEM-FRI divides the EEM signal into five regions (I,

308 II, III, IV and V; Fig. 3a). In the Tibet Plateau, these regions varied with changes in

309 intensity of the five marked fluorescence fractions between brackish lakes and the fresh

310 lakes. EEM-FRI results from the lakes were used to demonstrate CDOM fluorescence

311 characteristics. The excitation-emission area volumes  $\varphi_i$  ( $i = \text{I, II, III, IV, V}$ ) and their

312 proportion to total fluorescence intensity  $P_i$  ( $i = \text{I, II, III, IV, V}$ ) for the five different

313 regions are shown in Figure 4 (e and f), respectively. A significant difference (ANOVA

314  $p < 0.05$ ) of total fluorescence intensity  $\varphi_T$  was observed between the brackish and fresh

315 lakes.  $\varphi_T$  ranged from  $1.94 \times 10^8$  nm to  $3.5 \times 10^{10}$  nm for brackish lakes, having an

316 average of  $1.44 \times 10^{10}$  nm ( $\pm 8.1 \times 10^9$  SD), and it ranged from  $3.54 \times 10^8$  nm to  $3.5 \times$

317  $10^{10}$  nm for freshwater lakes, with an average of  $1.38 \times 10^{10}$  nm ( $\pm 7.9 \times 10^9$  SD). For

318 both lake types, the area volume of  $\varphi_i$  in the five integrated regions identified by EEM-

319 FRI were in the order of:  $\varphi_V$  (Humic-like)  $> \varphi_{III}$  (Fulvic-like)  $> \varphi_{IV}$  (Microbial protein-

320 like)  $> \varphi_I$  (Tyrosine-like)  $> \varphi_{II}$  (Tryptophan-like). This result indicates that the

321 allochthonous humic-like and fulvic-like materials are predominate in these DOM, and

322 the content of protein-like materials and phenolic compounds were low. Furthermore,

323 a significant difference for the fluorescence intensities of humic-like  $\varphi_V$  and fulvic-like

324  $\varphi_{III}$  was found in brackish lakes and fresh lakes (ANOVA,  $p < 0.05$ ). The fluorescence

325 intensities with  $\varphi_V$  accounting for  $P_V = 62.4\%$  ( $\pm 14.6$  SD) in brackish lakes ranged from

326 34.1% in Gemangcuo Lake (GMC) to 96.8% in Chuocuolong Lake (CCL). Then fresh

327 lakes recorded a range of 32.8% (Garencuo Lake; GRC-2) to 87.5% (Cuolongque Lake;

328 CLQ), having an average  $P_V$  of 53.7% ( $\pm 13.0$  SD). This result indicates that humic-like

329 substances both in brackish and fresh lakes dominated fluorescence intensities. In

330 addition, the  $\varphi_{III}$  (fulvic-like) fluorescence intensities also showed a significant



331 difference (ANOVA,  $p < 0.05$ ) between  $P_{III}$  in fresh lakes ( $24.8\% \pm 7.4$  SD) and those in  
 332 brackish lakes ( $15.9\% \pm 8.8$  SD). The fluorescence intensities for  $\varphi_{IV}$  (microbial  
 333 protein-like) accounted for a greater proportion in brackish lakes ( $P_{IV}$  of  $15.5\% \pm 8.2$   
 334 SD) than in fresh lakes ( $12.5\% \pm 6.8$  SD). These results demonstrated that the  
 335 fluorescence intensities of the five components  $\varphi_i$  ( $i = I, II, III, IV, V$ ) and the relative  
 336 proportions to the total fluorescence intensities  $P_i$  ( $i = I, II, III, IV, V$ ) differed in brackish  
 337 and fresh lakes.

338 [Insert Figure 4 about here]

### 339 3.4 Normalized EEM-FRI components and fluorescence indices

340 With various hydrological, geographical and climatic characteristics, the fluorescence  
 341 of CDOM components in different lakes shows spatial heterogeneity. The water  
 342 samples collected from each lake were combined to examine spatial variation in order  
 343 to eliminate the influence of spatial heterogeneity, the cumulative volumes beneath the  
 344 EEM ( $\varphi_i$ ) values were normalized to a DOC concentration of  $1 \text{ mg L}^{-1}$ . The average  
 345 normalized total fluorescence intensities  $\varphi_T$  in brackish lakes was  $1.1 \times 10^9 \text{ QSU-nm}^2$ –  
 346  $[\text{mg L}^{-1} \text{ C}]$  ( $\pm 8.8$  SD), with a maximum value of  $3.3 \times 10^9 \text{ QSU-nm}^2$ – $[\text{mg L}^{-1} \text{ C}]$  in  
 347 Gongzhucuo Lake (GZC) and a minimum value of  $4.8 \times 10^7 \text{ QSU-nm}^2$ – $[\text{mg L}^{-1} \text{ C}]$  in  
 348 Qinghaihu Lake (QHH). Results for the fresh lakes showed that  $\varphi_T$  ranged from  $2.1$   
 349  $\times 10^7 \text{ QSU-nm}^2$ – $[\text{mg L}^{-1} \text{ C}]$  in Tongzecuo Lake (TZC) to  $9.5 \times 10^9 \text{ QSU-nm}^2$ – $[\text{mg L}^{-1} \text{ C}]$   
 350 in Wurucuo Lake (WRC), having an average  $\varphi_T$  of  $3.3 \times 10^9 \text{ QSU-nm}^2$ – $[\text{mg L}^{-1} \text{ C}]$  ( $\pm 2.6$   
 351 SD). There was a significant difference of normalized total fluorescence intensities  $\varphi_T$   
 352 in brackish and fresh lakes (ANOVA,  $p < 0.001$ ), which is opposite to the non-  
 353 normalized EEM-FRI result in Figure 4e. This difference may be attributed to DOC  
 354 accumulation in terminal brackish lakes, having a prolonged hydraulic retention time



and irradiation, and the presence of a greater volume of colorless DOC (Table S1). By contrast, it can be seen that the inflow rivers of a certain lake generally showed lower DOC concentrations (Fig. S2). Although photochemistry due to strong UV-B caused the different composition of CDOM, allochthonous substances are important for the accumulation of DOC in brackish lakes.

In addition, the normalized volumes  $\phi_i$  in the five integrated regions identified by EEM-FRI also presented normalized  $\phi_V$  (humic-like),  $\phi_{III}$  (fulvic-like) and  $\phi_{IV}$  (microbial protein-like), these being more predominate in CDOM than  $\phi_I$  (tyrosine-like) and  $\phi_{II}$  (tryptophan-like). Percentage distributions ( $P_i$ ) of EEM-FRI extracted FDOM in brackish and fresh lakes also showed significant differences (ANOVA,  $p < 0.001$ ). Normalized humic-like ( $\phi_V$ ) and fulvic-like ( $\phi_{III}$ ) were terrestrial sources, accounting for  $P_{III+V} = 77.7\% (\pm 10.1 \text{ SD})$  in brackish lakes and  $77.7\% (\pm 7.3 \text{ SD})$  in fresh lakes. Protein-like fluorescence, including tyrosine-like and tryptophan-like ( $\phi_{I+II}$ ), recorded a greater proportion in brackish water ( $P_{I+II} = 6.47\% \pm 2.6 \text{ SD}$ ) than in fresh lakes ( $P_{I+II} = 22.3\% \pm 4.0 \text{ SD}$ ) (Fig. 5c and d). Although autochthonous and microbial occupied small proportions of normalized volumes  $\phi_T$ , FDOM in brackish lakes generally indicated more allochthonous inputs.

[Insert Figure 5 about here]

shown in Fig. 6, the average values of the fluorescence indices  $FI_{370}$  and  $FI_{310}$  introduced by McKnight et al. (2001) were derived to characterize CDOM sources in the Tibet Plateau (Fig. 6).  $FI_{370}$  in brackish lakes ranged from 0.11 (Peikucuo Lake; PKC) to 1.93 (Chuocuolong Lake; CCL), with a mean value of 0.64 ( $\pm 0.51 \text{ SD}$ );  $FI_{310}$  ranged from 0.58 (PKC) to 1.93 (Gemangcuo Lake; GMC), having a mean value of 1.14 ( $\pm 0.36 \text{ SD}$ ). In contrast, fresh lake results ranged from 0.11 (Taruocuo Lake; TRC) to 2.87 (Weizhi-1 Lake; WZ-1), with a mean value of 0.79 ( $\pm 0.75 \text{ SD}$ ) and from 0.57



(WZ-1) to 2.38 (La'angcuo Lake; LAC), with a mean value of  $1.04 (\pm 0.43 \text{ SD})$ , for  $FI_{370}$  and  $FI_{310}$ , respectively. Average  $FI_{370} (<1.4)$  and  $FI_{310} (>0.8)$  in most brackish and fresh lakes indicated that CDOM sources were derived from terrestrial humic-like substances and autochthonous biological activity. There may be no differences between  $FI_{310}$  and  $FI_{370}$ , signifying no difference for CDOM sources between brackish and fresh lakes (ANOVA,  $p>0.05$ ). However, average  $HIX$  ( $3.15 \pm 3.5$ ) in fresh lakes showed a higher degree of humification than in brackish lakes (average  $HIX$   $1.8 \pm 1.7$ ).

[Insert Figure 6 about here]

### 3.5 PCA of normalized EEM-FRI components

PCA (principal component analysis) was undertaken to calculate the relative scores of normalized cumulative volume  $\varphi_i$  by EEM-FRI, and to assess the spatial distributions of water samples in brackish and fresh lakes. Our results indicate that PCA factor 1 and factor 2 axes (Fig. 7) could explain 92.8% of total variance, and they account for 66.9% and 25.9%, respectively. The Kaiser-Meyer-Olkin result showed that the statistical magnitude was larger than 0.8, and that the five normalized EEM-FRI fluorescent components exhibited positive factor 1 loadings (Fig. 7a). Factor analysis showed PAC factor 1 and factor 2 to be associated with five cumulative volumes  $\varphi_i$  ( $i=I, II, III, IV, V$ ) in a linear formula. Factor 1 and factor 2 were expressed as:

$$\text{factor 1} = -0.543\varphi_I - 1.35\varphi_{II} + 0.788\varphi_{III} + 0.856\varphi_{IV} + 0.98\varphi_V$$

$$\text{factor 2} = 0.899\varphi_I + 1.78\varphi_{II} - 0.559\varphi_{III} - 0.636\varphi_{IV} - 0.774\varphi_V.$$

$\varphi_{III}$  (fulvic-like),  $\varphi_V$  (humic-like) and  $\varphi_{IV}$  (microbial protein-like) showed a positive factor 1 loading, and concurrently showed negative factor 2 loading. This correlation result indicated that PCA in our study could separate normalized cumulative volume  $\varphi_i$  by EEM-FRI into two groups: Group 1 ( $\varphi_{III}$ , fulvic-like;  $\varphi_V$ , humic-like;  $\varphi_{IV}$ , microbial



protein-like) and Group 2 ( $\phi_I$ , tyrosine-like;  $\phi_{II}$ , tryptophan-like). This finding was contrary to the results of Zhao et al. (2017), Yao et al. (2011) and Yamashita et al., (2010) from other water bodies. Differences in results from our study and previous investigations may be due to the majority of the microbial protein-like fluorescence of CDOM in lakes in our study being derived from terrestrial microbial decomposition. The spatial variation of PCA factors 1 and 2 scores for all water samples is shown in Figure 7b. Water samples from brackish lakes were mainly distributed in the range of -1 to 1 for both PCA factor scores. This finding confirms that the contributions of allochthonous substances (including microbial protein-like) were obvious in brackish lakes. Differences in FDOM results are likely to be due to spatial variations influencing terrestrial inputs from soil and microbial activities from plant decay. However, PCA scores from areas of fresh lakes were sporadic, signifying that normalized cumulative volume  $\phi_i$  were affected by regional hydrological and geographical lake conditions.

[Insert Figure 7 about here]

### 3.6 Correlation analysis of CDOM spectroscopic indices

In general, there was strong correlation between tyrosine-like  $\phi_I$  and tryptophan-like  $\phi_{II}$  in fresh ( $R^2=0.86$ ,  $N=135$ ;  $t$ -test,  $p<0.01$ ) and brackish lakes ( $R^2=0.80$ ,  $N=109$ ;  $t$ -test,  $p<0.01$ ), suggesting that they may have similar sources (Fig. 8a). A moderate correlation between  $\phi_I$  and microbial protein-like  $\phi_{IV}$  was observed in brackish lakes ( $R^2=0.70$ ,  $N=109$ ;  $t$ -test,  $p<0.01$ ), and a weak correlation was recorded in fresh lakes ( $R^2=0.57$ ,  $N=135$ ;  $t$ -test,  $p<0.01$ ) (Fig. 8b), demonstrating that parts of the two FRI fluorescent components may have some common sources in brackish lakes. However, strong correlations between tryptophan-like  $\phi_{II}$  and microbial protein-like  $\phi_{IV}$  were not observed (Fig. 8c), a finding that is consistent with the results of Chen et al. (2003) and



Zhao et al. (2017). This lack of correlation may be due to the sources of the three protein  
 fluorescence materials (tyrosine-like, tryptophan-like and microbial protein-like) being  
 independent in fresh lakes. Furthermore, EEM can be divided into two groups in the  
 PCA results (Fig. 7), and there was a positive correlation between the total normalized  
 cumulative volume  $\phi_{III+IV+V}$  and  $\phi_{I+II}$  ( $R^2 = 0.76$ ,  $N = 109$ ;  $t$ -test,  $p < 0.01$ ) in brackish  
 lakes (Fig. 8d). Then a weak correlation in fresh lakes ( $R^2 = 0.54$ ,  $N = 135$ ;  $t$ -test,  $p <$   
 0.01). It indicated that the autochthonous substances and they affected by  
 microorganism activity in brackish lakes was not strong. Arts et al. (2000) reported that  
 increasing salinity could limit the microbial activity by reduce the cell permeability. In  
 addition, moderate correlations between the  $a(350)$ ,  $FI_{370}$  and  $HIX$  were observed in the  
 fresh lakes ( $R^2 > 0.66$ ,  $N = 135$ ;  $t$ -test,  $p < 0.01$ ) (Fig. 8 e and f), showing that  $FI_{370}$  and  
 $HIX$  represented similar indications in CDOM sources for most fresh lakes. This result  
 was consistent with the findings of Zhang et al. (2010) and Zhao et al. (2016). In  
 brackish lakes,  $a(350)$  and  $HIX$  showed a more moderate correlation ( $R^2 = 0.65$ ,  $N = 109$ ;  
 $t$ -test,  $p < 0.01$ ).

[Insert Figure 8 about here]

### 3.7 Correlation between CDOM and water quality

Redundancy analysis (RDA) between water quality parameters for the brackish and  
 fresh lakes (Fig. 9) showed that the forward selected environment explanatory variables  
 (CDOM absorption and fluorescence;  $a(254)$ ,  $a(350)$ ,  $S_{275-295}$ ,  $SUVA_{254}$ ,  $M(E_{250}:E_{365})$ ,  
 $FI_{310}$ ,  $FI_{370}$ ,  $HIX$  and  $\phi_i$  ( $i = I, II, III, IV, V$ )), could explain the variability of species  
 variables (water quality parameters; DOC, Chl-a, TN, TP, salinity and turbidity).  
 Species–environment correlations of brackish and fresh lakes were 0.43 and 0.33,  
 respectively. For brackish lakes ( $N = 109$ ), the first two RDA axes accounted for 86.3%



of total water quality parameter variability (axis one, 48 %; axis two, 38.3 %).  
 Coefficients between environmental variables with RDA axes indicated that  $a(254)$ ,  
 $a(350)$  and  $HIX$  were correlated with CDOM, followed by  $M(E_{250}:E_{365})$  and  $S_{275-295}$ . For  
 the fresh lakes ( $N=135$ ), the first two RDA axes accounted for 82.4 % of total variability  
 (axis one, 66.7 %; axis two, 15.7 %).  $a(254)$ ,  $HIX$  and  $a(350)$  were correlated with water  
 quality, followed by  $FI_{370}$  and  $\phi_{IV}$ . The CDOM absorption  $a(254)$  can generally  
 characterize DOC aromaticity and CDOM concentration (Baker, 2001).

[Insert Figure 9 about here]

In addition, regression analysis was undertaken between DOC concentration and  
 normalized cumulative volume  $\phi_i$  ( $i=I, II, III, IV, V$ ) for all water samples (Table 2).  
 Salinity of the brackish lakes was divided into four parts: salinity  $>19\text{‰}$  (average EC  
 $23764 \mu\text{S cm}^{-1}$ ), salinity  $>7\text{‰}$  (average EC  $10945 \mu\text{S cm}^{-1}$ ), salinity  $>2\text{‰}$  (average EC  
 $5708 \mu\text{S cm}^{-1}$ ) and salinity  $<1\text{‰}$  (average EC  $2119 \mu\text{S cm}^{-1}$ ). Salinity  $<1\text{‰}$  was  
 consistent with that of fresh lakes (average EC  $586 \mu\text{S cm}^{-1}$ ). There were moderately  
 strong negative correlations between the normalized cumulative volume  $\phi_i$  ( $i=I, II, IV,$   
 $V$ ) and DOC concentration, with  $R^2$  ranging from 0.51 to 0.73. This result suggests that  
 parts of the FDOM components and DOC potentially derived from common sources in  
 brackish lakes (salinity  $>19\text{‰}$  or averaged EC  $23764 \mu\text{S cm}^{-1}$ ). In particular,  $R^2$  values  
 showed a consistent decreasing tendency with salinity (EC), suggesting that DOC with  
 high salinity (EC) was dominant with allochthonous substances. The link of the five  
 FDOM components to DOC was complicated due to various hydrological, geographical  
 and climatic characteristics.

[Insert Table 2 about here]

#### 4. Discussion

476 **4.1 The effect of EC/salinity**

477 Previous studies have reported that DOC concentrations in inland waters showed a  
478 decreased tendency with the prolongation of water residence times in humid regions  
479 due to prolonged photobleaching and possible dilution (Curtis and Adams, 1995;  
480 Spencer et al., 2012). For lakes in the study area having a long retention period (Table  
481 S1), brackish lakes were found to have higher DOC concentrations ( $35.69 \pm 43.52 \text{ mg}$   
482  $\text{L}^{-1}$ ) compared with fresh lakes ( $7.94 \pm 12.05 \text{ mg L}^{-1}$ ) (Table 1). Substantial variations  
483 for both DOC and CDOM spectroscopic parameters were also observed between the  
484 fresh and brackish lakes (ANOVA,  $p < 0.05$ ) (Table 1 and Fig. 3). Previous investigations  
485 have attributed this pattern to evapo-concentrated and accumulation processes in semi-  
486 arid regions (Twardowski and Donaghay, 2002; Song et al., 2013; Wen et al., 2016).  
487 However, the affined characteristics of brackish lakes in our study area could be due to  
488 a weak connection between salinity (EC) and DOC (un-exhibited;  $R^2 = 0.3$ ,  $t$ -test,  
489  $p < 0.01$ ). Comparably, opposite results from brackish lakes in the northeastern plain  
490 ( $R^2 = 0.93$ ,  $p < 0.01$ ; Zhao et al., 2016) and on the Inner Mongolia Plateau ( $R^2 = 0.72$ ,  
491  $p < 0.01$ ; Wen et al., 2016) have been previously noted. Generally, organic carbon with  
492 different sources (allochthonous or autochthonous) and composition may result in  
493 different relationships existing between DOC and salinity (EC) (Spencer et al., 2012).  
494 This indicated that regional hydrogeological and climatic conditions may play an

495 important role in driving DOC variability in brackish lakes.

496 Although the lakes in the study area have high spatial heterogeneity, decreasing  
497 salinity generally showed a consistent tendency of DOC concentrations (Fig. 2b).  
498 Furthermore, salinity was divided into four groups ( $>19\text{‰}$ ;  $>7\text{‰}$ ;  $>2\text{‰}$ ;  $>1\text{‰}$ ) in  
499 brackish lakes (Table 2). The normalized cumulative volume  $\varphi_i$  ( $\varphi_I$ ,  $\varphi_{II}$ ,  $\varphi_{IV}$  and  $\varphi_V$ ) of  
500 water samples with a salinity  $>19\text{‰}$  (average EC  $23764 \mu\text{S cm}^{-1}$ ) by EEM-FRI showed



501 moderate correlations with DOC concentrations ( $R^2$  ranged from 0.52 to 0.73).  $R^2$   
502 correlation values showed a consistent decreasing tendency with salinity or EC. Based  
503 on previous research which showed brackish lakes to always contain higher  
504 concentrations of DOC than freshwater lakes in arid regions, this result may reflect  
505 water residence times and DOM accumulation. DOM, along with other nutrients, could  
506 accumulate via soil leaching and runoff passing through various landscapes (Song et al.,  
507 2013). These DOM could be available for the microorganisms and sink to the bottom,  
508 or be transformed into inorganic carbon (including  $\text{CO}_2$ ) (Cole et al., 2007; Tranvik et  
509 al., 2009). Increasing salinity (EC) could increase DOM solubility, resulting in an  
510 impact on microbial activity due to a decrease of osmotic potential (Mavi et al., 2012).  
511 Likewise, saturating small humic-like molecules formed colloidal particles which could  
512 continue to form macromolecular structures (globular aggregates and ring-like) in high  
513 ionic strength environments (Chin et al., 1998; Myneni et al., 1999; Zhao et al., 2016).  
514 Therefore, DOC accumulates in brackish (terminal) waters at significantly higher rates  
515 than those in fresh (open) waters (Duarte et al., 2005; Song et al., 2013).



516 A higher humic-like averaged percentage ( $P_V$  60.2%) by normalized EEM-FRI  
517 was presented in brackish lakes compared with freshwater lakes (51.8%) (Fig. 5),  
518 signifying a greater formation of macromolecular structures of humic-like substances.  
519 These processes could account for DOC and nutrients accumulating in terminal  
520 brackish lakes. RDA results also indicated that environmental variables (CDOM  
521 absorption and fluorescence) showed a relatively more positive correlation with water  
522 quality in brackish lakes than in fresh lakes (Fig. 9). Zhao et al. (2016) reported that the  
523 formed macromolecular structures of humic-like substances in brackish aquatic  
524 environments can regulate the solubility of heavy metals and organic pollutants in water.  
525 For areas of brackish lakes in the study site, elevated DOC concentrations could be



526 attributed to evapo-concentration and accumulation due to long residence times.

#### 527 4.2 The effect of solar radiation/ elevation

528 In these synchronous processes (arid environment, terminal lakes and terrestrial inputs),  
 529 it is also important to highlight that these lakes receive higher levels of ultraviolet  
 530 radiation due to increasing altitude and a thin atmosphere compared to other studies  
 531 (Ren et al., 1997) (Fig. 1c). These attributes result in increased exposure to sunlight, an  
 532 increase in water residence times and strong UV radiation with an increase of altitude.  
 533 These factors may have an important influence on the photochemical oxidation  
 534 processes of DOC/CDOM and the mineralization of DOC (Duarte et al., 2005; Tobias  
 535 and Bohlke, 2011). Among the 63 lakes ( $N=224$ ), the average  $M(E_{250}:E_{365})$  ( $28.3 \pm 20.3$ ),  
 536  $S_{275-295}$  ( $0.0380 \pm 0.009 \text{ nm}^{-1}$ ) and  $SUVA_{254}$  ( $1.47 \pm 2.55 \text{ mg C}^{-1} \text{ m}^{-1}$ ) in the brackish  
 537 lakes ( $N=109$ ) were distinctly different from fresh lake results ( $N=135$ ):  $a(350)$  ( $1.74 \pm$   
 538  $1.99 \text{ m}^{-1}$ ),  $M(E_{250}:E_{365})$  ( $16.27 \pm 20.6$ ),  $S_{275-295}$  ( $0.0324 \pm 0.01 \text{ nm}^{-1}$ ) and  $SUVA_{254}$  ( $2.29$   
 539  $\pm 1.36$ ), respectively. This pattern is similar to that reported by Boehme et al. (2004) in  
 540 the Gulf of Mexico. In contrast with previous research indicating that brackish (terminal)  
 541 lakes always contain terrestrial DOM accumulation, our results show that they were  
 542 provided with low aromatic moieties of CDOM and average molecular weight of DOC  
 543 compared within fresh lakes (Helms et al., 2008; Gonnelli et al., 2013). Results also  
 544 highlighted significant differences in total fluorescence intensities  $\phi_T$  between brackish  
 545 lakes ( $1.44 \times 10^{10} \pm 8.1 \times 10^9 \text{ nm}$ ) and fresh lakes ( $1.38 \times 10^{10} \pm 7.9 \times 10^9 \text{ nm}$ ) (ANOVA,  
 546  $p < 0.001$ ) (Fig. 5 and Fig. 6), respectively. However, we found that the average  
 547 normalized total fluorescence intensities  $\phi_T$  between brackish lakes ( $1.1 \times 10^9 \pm 8.8 \text{ QSU-}$   
 548  $\text{nm}^2 \cdot [\text{mg L}^{-1} \text{ C}]$ ) and fresh lakes ( $3.3 \times 10^9 \pm 2.6 \text{ QSU-} \text{nm}^2 \cdot [\text{mg L}^{-1} \text{ C}]$ ) showed opposite  
 549 vitiation tendency when the  $\phi_T$  was normalized to a DOC concentration of  $1 \text{ mg L}^{-1}$ .  
 550 This finding may account for relatively higher colorless DOC present in the brackish



551 lakes compared with the fresh lakes, a finding linked to solar radiation and prolonged  
552 hydraulic retention time (Table S1).

553 In order to evaluate the influence of solar irradiance to CDOM optical  
554 characteristics (Fig. 10), solar irradiance was divided into three groups ( $>2900$  h;  $>2800$   
555 h;  $>2700$  h) based on the consistent result of decreasing tendency between elevation  
556 (solar radiation) and DOC concentration (Fig. 2). Strong solar radiance and time could  
557 accelerate chromophores associated with high molecular weight being destroyed by  
558 chemical bond rupture into low molecular weight pools in photolysis processes with a  
559 prolonged hydraulic retention time and intensive solar radiation (McKnight et al., 2001).  
560 However, for water samples with a solar radiance  $>2900$  h (averaged solar irradiance),  
561 DOC recorded a moderate positive correlation with  $a(254)$  concentrations ( $R^2=0.73$ ,  $t$ -  
562 test,  $p<0.01$ ), and a correlation with  $FI_{370}$  ( $R^2=0.50$ ,  $t$ -test,  $p<0.01$ ). This indicated that,  
563 in areas of the Tibet Plateau with intensive UV-B radiation (solar irradiance,  $>2900$  h),  
564 parts of the colored DOM (mainly from allochthonous inputs) have similar sources with  
565 DOC. In addition, the PCA result of normalized cumulative volume  $\phi_i$  by EEM-FRI in  
566 this study exhibited that  $\phi_{IV}$  (microbial protein-like) was consistent with  $\phi_V$  (humic-like)  
567 and  $\phi_{III}$  (fuvic-like), signifying that they have common sources (Fig. 7). A positive  
568 correlation between the total normalized cumulative volume  $\phi_{III\&IV\&V}$  and  $\phi_{I\&II}$  ( $R^2=$   
569  $0.76$ ,  $N=109$ ;  $t$ -test,  $p<0.01$ ) in brackish lakes also demonstrated that microbial protein-  
570 like FDOM in these lakes had high DOC concentrations associated with products from  
571 terrestrial microbial decomposition (Fig. 8d). Zhang et al. (2013) identified correlations  
572 between total bacterial community structure and altitude in Tibet, and they did not find  
573 more microorganism usually dominate in other lake environments, even though a  
574 relative high average percentage of  $P_{IV}$  (brackish 15.8%; freshwater 13.3%) were  
575 identified for normalized cumulative volume (Fig. 5). In the Tibet Plateau, intensive



576 solar radiance has the potential to enhance photochemical degradation of allochthonous  
577 CDOM and high molecular weight CDOM, resulting in an increase in absorption  
578 parameters with the production of low molecular weight CDOM. These findings are  
579 contrary to those recorded from rivers in intermontane plateaus in the USA (Spencer et  
580 al., 2012), lakes in the Songnen Plain, China (Song et al., 2013), Hulun Lake, China  
581 (Wen et al., 2016) and basin rivers in China (Zhao et al., 2016). In arid and semi-arid  
582 regions, brackish lakes commonly support highly active biological communities which  
583 can actively break down refractory organic matter into DOC and accumulate in waters  
584 (Wen et al., 2016). However, due to strong UV-B radiation and terminal lakes in the  
585 Tibet Plateau, long sunlight duration may result in photobleaching of CDOM which  
586 will limit microbial activities and increase mineralization of DOC (Granéli et al., 1996;  
587 Duarte et al., 2005). These Characteristics characters result in CDOM and DOC in  
588 brackish lakes in the study area being similar to that in marine environments. Zhang et  
589 al. (2013) reported that the majority of lakes in Tibet were affiliated with SAKIT-III  
590 clade, similar to observations from Chesapeake Bay bacterio plankton. These findings  
591 show that solar radiation has a non-negligible effect on CDOM photo-absorption  
592 characteristics, and that it contributes to DOC variability and fate. In addition, a  
593 comparatively prolonged hydraulic retention time (Duarte et al., 2005) and terrestrial  
594 allochthonous inputs could cause higher DOC production and accumulation.

595 **[Insert Figure 10 about here]**

#### 596 **4.3 Effects of land-cover variation on lakes**

597 Land-cover types within and around each lake affect soil runoff and leaching, having  
598 an important effect on CDOM inputs and nutrient levels. These effects result in obvious  
599 differences in physicochemical properties between the lakes (Bai et al., 2008; Heinz et



al., 2015; Song et al., 2013). In particular, for water samples dominated by  
allochthonous substances in terminal lakes, spatial variations influenced terrestrial  
inputs from soil and microbial activities due to plant decay. The land-cover in the basin  
can also affect CDOM components and FDOM with similar climatic and hydrological  
conditions. In order to acquire the integrated land-cover area of each basin, 20 basins  
(B1-B20) were extracted using a 30 m resolution DEM (Digital Elevation Model;  
<http://www.gscloud.cn/>). The proportion of different land use types to total basin area  
is shown in Figure S2. In the Tibet Plateau, grass with plentiful organic-rich ecosystems  
were the major land-cover types, accounting for amounts of total basin area (Fig. S2).  
CDOM optical parameters of lake samples in each basin were averaged to analyze the  
influence of land-cover, results showing a moderate correlation between DOC and  
normalized humic-like  $\phi_V$  for 20 basins ( $R^2=0.54$ ,  $t$ -test,  $p<0.01$ ; Fig. 11). Due to the  
grass area accounting for amounts of basins (Fig. S3), normalized  $\phi_{III}$ ,  $\phi_{IV}$  and  $\phi_V$  in  
basins with large grass areas (average area 14876 km<sup>2</sup>;  $N=10$  basins) exhibited higher  
values than in basins with small grass areas (averaged area 1976 km<sup>2</sup>;  $N=10$  basins)  
(ANOVA,  $p<0.05$ ). Similar results were also found for forest and unused land, although  
they accounted for small proportions of total area (Fig. 11). The Tibet Plateau is located  
in an arid climatic zone with low rainfall, and the impoundment of lakes mainly depends  
on surface runoff. Grasslands and forests were characterized by high nitrogen and  
organic matter export rates (Bai et al., 2008; Heinz et al., 2015). High DOC  
concentrations in the lake waters highlights the organic-rich nature of these ecosystems  
(Zheng et al., 2015). As a result of climatic and geographical conditions, these  
environment factors may change the optical characteristic of CDOM and water quality  
in the Tibet Plateau.



## 625 **5. Conclusions**

626 Little is currently known about CDOM fluorescence and its relationship with water  
 627 quality in lakes across the Tibet Plateau. This area has a unique environmental condition  
 628 with strong ultraviolet radiation and low anthropogenic impact. In this study, EEM-FRI  
 629 was applied to characterize CDOM from 63 lakes ( $N=244$ ) **under spatial variation**  
 630 **between brackish lakes (salinity>1‰) and fresh lakes (salinity<1‰).** Significant  
 631 differences of CDOM absorption parameters, normalized  $\phi_T$  and DOC concentrations  
 632 were found between the two lake types (ANOVA,  $p<0.05$ ), indicating lower average  
 633 molecular weight of DOM in brackish lakes.

634 Although the terrestrial component ( $\phi_{III}$  and  $\phi_V$ ) accounted for large amounts of  
 635 fluorescence, PCA results indicated that the majority of microbial protein-like  
 636 fluorescence  $\phi_{IV}$  of CDOM in the lakes derived from terrestrial microbial  
 637 decomposition products. This was attributed to DOC accumulation in terminal brackish  
 638 lakes having a prolonged hydraulic retention time and solar radiation. In addition,  
 639 correlations between average DOC concentrations and  $a(254)$  in annual total sunshine  
 640 hours  $> 2900$  h or salinity  $>19‰$  (averaged EC,  $23764\mu\text{s cm}^{-1}$ ) were identified, while  
 641  $R^2$  values of regression analysis had a decreasing tendency with sunshine hours and  
 642 salinity, respectively. Findings from our study also demonstrated that CDOM  
 643 components were affected by spatial variation in land-cover (mainly grass) (ANOVA,  
 644  $p<0.05$ ), with a moderate relationship between average normalized  $\phi_V$  and DOC  
 645 concentration from 20 basins ( $R^2=0.54$ ,  $t$ -test,  $p<0.01$ ). These results demonstrate that  
 646 salinity, solar hours and land-cover may contribute to CDOM and DOC properties. The  
 647 EEM-FRI method was also shown to be very useful for evaluating the spatial dynamics  
 648 of FDOM components.

## 649 **Acknowledgments**



650 The research was jointly supported by the “One Hundred Talents” program from  
651 Chinese Academy of Sciences, and the National Natural Science Foundation of China  
652 (41730104). The authors thank all staff in Northeast Institute of Geography and  
653 agricultural ecology of Chinese Academy of Sciences for their persistent assistance  
654 with both field sampling and laboratory analysis. The authors also would like to thank  
655 anonymous reviewers for their instructive and valuable comments that really  
656 strengthened this manuscript.

657

## 658 **References**

659 APHA, AWWA and WEF,: Standard Methods for the Examination of Water and  
660 Wastewater, American Public Health Association, Washington DC, 1998.

661 Arts, M. T., Robarts, R. D., Kasai, F., Waiser, M. J., Tumber, V. P., Plante, A. J., Rai,  
662 H., and Lange, H. J.: The attenuation of ultraviolet radiation in high dissolved  
663 organic carbon waters of wetlands and lakes on the northern Great Plains,  
664 Limnology and Oceanography, 45(2), 292-299,  
665 <https://doi.org/10.4319/lo.2000.45.2.0292>, 2000.

666 Baker, A.: Fluorescence excitation–Emission matrix characterization of some sewage-  
667 impacted rivers, Environmental Science & Technology, 35(5), 948-953,  
668 <https://doi.org/10.1021/es000177t>, 2001.

669 Battin, T. J., Luyssaert, S., Kaplan, L. A., Aufdenkampe, A. K., Richter, A., and Tranvik,  
670 L. J.: The boundless carbon cycle, Nature Geoscience, 2(9), 598,  
671 <https://doi.org/10.1038/ngeo618>, 2009.

672 Boehme, J., Coble, P., Conmy, R., and Stovall-Leonard, A.: Examining CDOM



- 673 fluorescence variability using principal component analysis: seasonal and regional  
674 modeling of three-dimensional fluorescence in the Gulf of Mexico, *Marine*  
675 *Chemistry*, 89(1-4), 3-14, <https://doi.org/10.1016/j.marchem.2004.03.019>, 2004.
- 676 Carlson, C. A., Hansell, D. A., and Tamburini, C. (Eds): DOC persistence and its fate  
677 after export within the ocean interior, *Microbial Carbon Pump in the Ocean*, Jiao  
678 N, Azam F, Sanders S, Washington DC, 57–59, 2011.
- 679 Chen, W., Westerhoff, P., Leenheer, J. A., and Booksh, K.: Fluorescence excitation-  
680 emission matrix regional integration to quantify spectra for dissolved organic  
681 matter, *Environmental science & technology*, 37(24), 5701-5710.  
682 <https://doi.org/10.1021/es034354c>, 2003.
- 683 Chin, W. C., Orellana, M. V., and Verdugo, P.: Spontaneous assembly of marine  
684 dissolved organic matter into polymer gels, *Nature*, 391(6667), 568,  
685 <https://doi.org/10.1038/35345>, 1998.
- 686 Cole, J. J., Prairie, Y. T., Caraco, N. F., McDowell, W. H., Tranvik, L. J., Striegl, R. G.,  
687 Duarte, C. M., Kortelainen, P., Downing, J. A., Middelburg, J. J., and Melack, J.:  
688 Plumbing the global carbon cycle: integrating inland waters into the terrestrial  
689 carbon budget, *Ecosystems*, 10(1), 172-185. [https://doi.org/10.1007/s10021-006-](https://doi.org/10.1007/s10021-006-9013-8)  
690 9013-8, 2007.
- 691 Coble, P. G.: Characterization of marine and terrestrial DOM in seawater using  
692 excitation-emission matrix spectroscopy, *Marine chemistry*, 51(4), 325-346,  
693 [https://doi.org/10.1016/0304-4203\(95\)00062-3](https://doi.org/10.1016/0304-4203(95)00062-3), 1996.
- 694 Curtis, P. J., and Adams, H. E.: Dissolved organic matter quantity and quality from  
695 freshwater and saltwater lakes in east-central Alberta, *Biogeochemistry*, 30(1), 59-  
696 76, <https://doi.org/10.1007/BF02181040>, 1995.



- 707 Duarte, C. M., and Prairie, Y. T.: Prevalence of heterotrophy and atmospheric CO<sub>2</sub>  
708 emissions from aquatic ecosystems, *Ecosystems*, 8(7), 862-870,  
709 <https://doi.org/10.1007/s10021-005-0177-4>, 2005.
- 710 Falkowski, P., Scholes, R. J., Boyle, E., Canadell, J., Canfield, D., Elser, J., Gruber, N.,  
711 Hibbard, K., Högberg, P., Linder, S., Mackenzie, F. T., Moore III, B., Pedersen,  
712 T., Rosenthal, Y., Seitzinger, S., Smetacek, V., and Steffen, W.: The global carbon  
713 cycle: a test of our knowledge of earth as a system, *science*, 290(5490), 291-296,  
714 <https://doi.org/10.1126/science.290.5490.291>, 2000.
- 715 Gonnelli, M., Vestri, S., and Santinelli, C.: Chromophoric dissolved organic matter and  
716 microbial enzymatic activity. A biophysical approach to understand the marine  
717 carbon cycle, *Biophysical chemistry*, 182, 79-85,  
718 <https://doi.org/10.1016/j.bpc.2013.06.016>, 2013.
- 719 Granéli, W., Lindell, M., and Tranvik, L.: Photo-oxidative production of dissolved  
720 inorganic carbon in lakes of different humic content, *Limnology and  
Oceanography*, 41(4), 698-706, <https://doi.org/10.4319/lo.1996.41.4.0698>, 1996.
- 721 Hedges, J. I.: Global biogeochemical cycles: progress and problems, *Marine  
chemistry*, 39(1-3), 67-93, [https://doi.org/10.1016/0304-4203\(92\)90096-S](https://doi.org/10.1016/0304-4203(92)90096-S), 1992.
- 722 Heinz, M., Graeber, D., Zak, D., Zwirnmann, E., Gelbrecht, J., and Pusch, M. T.:  
723 Comparison of organic matter composition in agricultural versus forest affected  
724 headwaters with special emphasis on organic nitrogen, *Environmental science &  
technology*, 49, 2081-2090, <https://doi.org/10.1021/es505146h>, 2015.
- 725 Helms, J. R., Stubbins, A., Ritchie, J. D., Minor, E. C., Kieber, D. J., and Mopper, K.:  
726 Absorption spectral slopes and slope ratios as indicators of molecular weight,  
727 source, and photobleaching of chromophoric dissolved organic matter, *Limnology*



721 and Oceanography, 53(3), 955-969, <https://doi.org/10.4319/lo.2008.53.3.0955>,  
722 2008.

723 Huguet, A., Vacher, L., Relexans, S., Saubusse, S., Froidefond, J.M., and Parlanti, E.:  
724 Properties of fluorescent dissolved organic matter in the Gironde Estuary, Organic  
725 Geochemistry, 40(6), 706-719, <https://doi.org/10.1016/j.orggeochem.2009.03.002>,  
726 2009.

727 Kowalczyk, P., Cooper, W. J., Durako, M. J., Kahn, A. E., Gonsior, M., and Young, H.:  
728 Characterization of dissolved organic matter fluorescence in the South Atlantic  
729 Bight with use of PARAFAC model: Relationships between fluorescence and its  
730 components, absorption coefficients and organic carbon concentrations, Marine  
731 Chemistry, 118(1-2), 22-36, <https://doi.org/10.1016/j.marchem.2009.10.002>,  
732 2010.

733 Jiao, N., Herndl, G. J., Hansell, D. A., Benner, R., Kattner, G., Wilhelm, S. W.,  
734 Kirchman, D. L., Weinbauer, M. G., Luo, T., Chen, F., and Azam, F.: Microbial  
735 production of recalcitrant dissolved organic matter: long-term carbon storage in  
736 the global ocean, Nature Reviews Microbiology, 8(8), 593,  
737 <https://doi.org/10.1038/nrmicro2386>, 2010.

738 Lawaetz, A. J., and Stedmon, C. A.: Fluorescence intensity calibration using the Raman  
739 scatter peak of water, Applied spectroscopy, 63(8), 936-940,  
740 <https://doi.org/10.1366/000370209788964548>, 2009.

741 Liu, X., and Chen, B.: Climatic warming in the Tibetan Plateau during recent decades,  
742 International journal of climatology, 20(14), 1729-1742,  
743 [https://doi.org/10.1002/1097-0088\(20001130\)20:14<1729::AID-](https://doi.org/10.1002/1097-0088(20001130)20:14<1729::AID-JOC556>3.0.CO;2-Y)  
744 JOC556>3.0.CO;2-Y, 2000.



- 745 Mavi, M. S., Marschner, P., and Chittleborough, D. J.: Salinity and sodicity affect soil  
746 respiration and dissolved organic matter dynamics differentially in soils varying  
747 in texture, Soil biology and biochemistry, 45, 8-13,  
748 <https://doi.org/10.1016/j.soilbio.2011.10.003>, 2012.
- 749 McKnight, D. M., Boyer, E. W., Westerhoff, P. K., Doran, P. T., Kulbe, T., and  
750 Andersen, D. T.: Spectrofluorometric characterization of dissolved organic matter  
751 for indication of precursor organic material and aromaticity, Limnology and  
752 Oceanography, 46(1), 38-48, <https://doi.org/10.4319/lo.2001.46.1.0038>, 2001.
- 753 Myneni, S. C. B., Brown, J. T., Martinez, G. A., and Meyer-Ilse, W.: Imaging of humic  
754 substance macromolecular structures in water and soils, Science, 286(5443),  
755 1335-1337, <https://doi.org/10.1126/science.286.5443.1335>, 1999.
- 756 Qin, J., Yang, K., Liang, S., and Guo, X.: The altitudinal dependence of recent rapid  
757 warming over the Tibetan Plateau, Climatic Change, 97(1-2), 321,  
758 <https://doi.org/10.1007/s10584-009-9733-9>, 2009.
- 759 Ran, L. S., X. X. Lu, H. G. Sun, Han, J. T., Li, R. H., and Zhang, J.M.: Spatial and  
760 seasonal variability of organic carbon transport in the Yellow River, China,  
761 Journal of Hydrology, 498, 76-88, <https://doi.org/10.1016/j.jhydrol.2013.06.018>,  
762 2013.
- 763 Ren, P. B. C., Sigernes, F., and Gjessing, Y.: Ground-based measurements of solar  
764 ultraviolet radiation in Tibet: Preliminary results, Geophysical research  
765 letters, 24(11), 1359-1362, <https://doi.org/10.1029/97GL01319>, 1997.
- 766 Singh, S., D'Sa, E. J., and Swenson, E. M.: Chromophoric dissolved organic matter  
767 (CDOM) variability in Barataria Basin using excitation–emission matrix (EEM)



768 fluorescence and parallel factor analysis (PARAFAC), Science of the total  
769 environment, 408(16), 3211-3222,  
770 <https://doi.org/10.1016/j.scitotenv.2010.03.044>, 2010.

771 Song, K. S., Zang, S. Y., Zhao, Y., Li, L., Du, J., Zhang, N. N., Wang, X. D., Shao, T.  
772 T., Guan, Y., and Liu, L.: Spatiotemporal characterization of dissolved carbon for  
773 inland waters in semi-humid/semi-arid region, China, Hydrology and Earth  
774 System Sciences, 17(10), 4269-4281, <https://doi.org/10.5194/hess-17-4269-2013>,  
775 2013.

776 Song, K., Wang, M., Du, J., Yuan, Y., Ma, J. H., Wang, M., and Mu, G. Y.:  
777 Spatiotemporal variations of lake surface temperature across the Tibetan Plateau  
778 using MODIS LST product, Remote Sensing, 8(10), 854,  
779 <https://doi.org/10.3390/rs8100854>, 2016.

780 Spencer, R. G., Butler, K. D., and Aiken, G. R.: Dissolved organic carbon and  
781 chromophoric dissolved organic matter properties of rivers in the USA, Journal of  
782 Geophysical Research: Biogeosciences, 117(G3), G03001,  
783 <https://doi.org/10.1029/2011JG001928>, 2012.

784 Stedmon, C. A., Markager, S., and Bro, R.: Tracing dissolved organic matter in aquatic  
785 environments using a new approach to fluorescence spectroscopy, Marine  
786 Chemistry, 82(3-4), 239-254, [https://doi.org/10.1016/S0304-4203\(03\)00072-0](https://doi.org/10.1016/S0304-4203(03)00072-0),  
787 2003.

788 Tranvik, L. J., Downing, J. A., Cotner, J. B., Loiselle, S. A., Striegl, R. G., Ballatore,  
789 T. J., Dillon, P., Finlay, K., Fortino, K., Knoll, L. B., Kortelainen, P. L., Kutser,  
790 T., Larsen, S., Laurion, I., Leech, D. M., McCallister, S. L., McKnight, D. M.,  
791 Melack, J. M., Overholt, E., Porter, J. A., Prairie, Y., Renwick, W. H., Roland, F.,



- 792 Sherman, B. S., Schindler, D. W., Sobek, S., Tremblay, A., Vanni, M. J.,  
793 Verschoor, A. M., Wachenfeldt, E. V., and Weyhenmeyer, G. A.: Lakes and  
794 reservoirs as regulators of carbon cycling and climate, *Limnology and*  
795 *Oceanography*, 54(6part2), 2298-2314,  
796 [https://doi.org/10.4319/lo.2009.54.6\\_part\\_2.2298](https://doi.org/10.4319/lo.2009.54.6_part_2.2298), 2009.
- 797 Tobias, C., and Böhlke, J. K.: Biological and geochemical controls on diel dissolved  
798 inorganic carbon cycling in a low-order agricultural stream: Implications for reach  
799 scales and beyond, *Chemical Geology*, 283(1-2), 18-30,  
800 <https://doi.org/10.1016/j.chemgeo.2010.12.012>, 2011.
- 801 Twardowski, M. S., and Donaghay, P. L.: Photobleaching of aquatic dissolved  
802 materials: Absorption removal, spectral alteration, and their interrelationship,  
803 *Journal of Geophysical Research: Oceans*, 107(C8), 6-1-6-12,  
804 <https://doi.org/10.1029/1999JC000281>, 2002.
- 805 Waiser, M. J., and Robarts, R. D.: Changes in composition and reactivity of  
806 allochthonous DOM in a prairie saline lake, *Limnology and Oceanography*, 45(4),  
807 763-774, <https://doi.org/10.4319/lo.2000.45.4.0763>, 2000.
- 808 Weishaar, J. L., Aiken, G. R., Bergamaschi, B. A., Fram, M. S., Fujii, R., and Mopper,  
809 K.: Evaluation of specific ultraviolet absorbance as an indicator of the chemical  
810 composition and reactivity of dissolved organic carbon, *Environmental science &*  
811 *technology*, 37(20), 4702-4708, <https://doi.org/10.1021/es030360x>, 2003.
- 812 Wen, Z. D., Song, K. S., Zhao, Y., Du, J., and Ma, J. H.: Influence of environmental  
813 factors on spectral characteristics of chromophoric dissolved organic matter  
814 (CDOM) in Inner Mongolia Plateau, China, *Hydrology and Earth System Sciences*,  
815 20(2), 787, <https://doi.org/10.5194/hess-20-787-2016>, 2016.



- 816 Yao, X., Y. L. Zhang, G. W. Zhu, Qin, B. Q., Feng, L. Q., Cai, L. L., and Gao, G.:  
817 Resolving the variability of CDOM fluorescence to differentiate the sources and  
818 fate of DOM in Lake Taihu and its tributaries, *Chemosphere*, 82, 145-155,  
819 <https://doi.org/10.1016/j.chemosphere.2010.10.049>, 2011.
- 820 Yamashita, Y., Maie, N., Briceno, H., and Jaffé, R.: Optical characterization of  
821 dissolved organic matter in tropical rivers of the Guayana Shield, Venezuela,  
822 *Journal of Geophysical Research: Biogeosciences*, 115(G1),  
823 <https://doi.org/10.1029/2009JG000987>, 2010.
- 824 Zhang, R., Wu, Q., Piceno, Y. M., Desantis, T. Z., Saunders, F. M., Andersen, G. L.,  
825 and Liu, W. T.: Diversity of bacterioplankton in contrasting Tibetan lakes revealed  
826 by high-density microarray and clone library analysis, *FEMS microbiology*  
827 *ecology*, 86(2), 277-287, <https://doi.org/10.1111/1574-6941.12160>, 2013.
- 828 Zhang, G., Xie, H., Kang, S., Yi, D., and Ackley, S. F.: Monitoring lake level changes  
829 on the Tibetan Plateau using ICESat altimetry data (2003–2009), *Remote Sensing*  
830 *of Environment*, 115(7), 1733-1742, <https://doi.org/10.1016/j.rse.2011.03.005>,  
831 2011.
- 832 Zhang, Y., Yin, Y., Feng, L., Zhu, G., Shi, Z., Liu, X., and Zhang, Y.: Characterizing  
833 chromophoric dissolved organic matter in Lake Tianmuhu and its catchment basin  
834 using excitation-emission matrix fluorescence and parallel factor analysis, *Water*  
835 *research*, 45(16), 5110-5122, <https://doi.org/10.1016/j.watres.2011.07.014>, 2011.
- 836 Zhang, Y. L., E. L. Zhang, Y. Yin, Dijk, M. A.V., Feng, L. Q., Shi, Z. Q., Liu, M. L.,  
837 and Qin, B. Q.: Characteristics and sources of chromophoric dissolved organic  
838 matter in lakes of the Yungui Plateau, China, differing in trophic state and altitude,  
839 *Limnology and Oceanography*, 55, 2645–2659,



840 <https://doi.org/10.4319/lo.2010.55.6.2645>, 2010.

841 Zhao, Y., Song, K., Shang, Y., Shao, T., Wen, Z., and Lv, L.: Characterization of  
 842 CDOM of river waters in China using fluorescence excitation-emission matrix and  
 843 regional integration techniques, Journal of Geophysical Research: Biogeosciences,  
 844 122(8): 1940-1953, <https://doi.org/10.1002/2017JG003820>, 2017.

845 Zhao, Y., Song, K., Wen, Z., Li, L., Zang, S., Shao, T., Li, S., and Du, J.: Seasonal  
 846 characterization of CDOM for lakes in semiarid regions of Northeast China using  
 847 excitation–emission matrix fluorescence and parallel factor analysis (EEM–  
 848 PARAFAC), Biogeosciences, 13(5), 1635-1645, [https://doi.org/10.5194/bg-13-](https://doi.org/10.5194/bg-13-1635-2016)  
 849 1635-2016, 2016.

850 Zhou, Y., Jeppesen, E., Zhang, Y., Shi, K., Liu, X., and Zhu, G.: Dissolved organic  
 851 matter fluorescence at wavelength 275/342 nm as a key indicator for detection of  
 852 point-source contamination in a large Chinese drinking water lake, Chemosphere,  
 853 144, 503-509, <https://doi.org/10.1016/j.chemosphere.2015.09.027>, 2016.

854

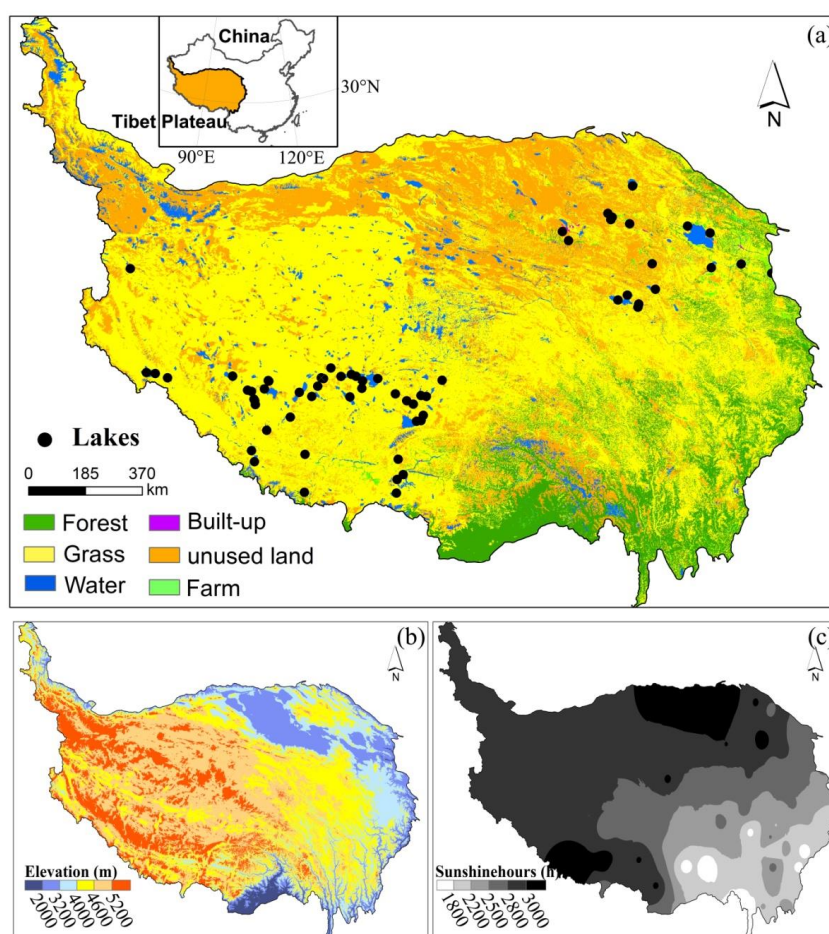
855

856

857



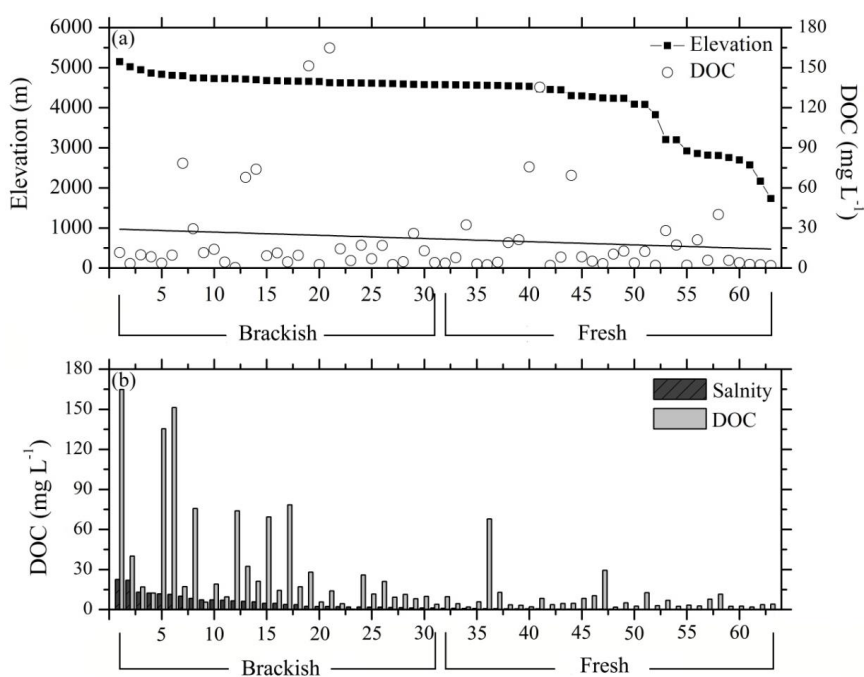
858 **Figure 1 (a) Map of sampling** locations from lakes in Tibet Plateau with various land  
 859 use/land cover types; (b) the elevation (m) of Tibet Plateau; (c) sunshine duration  
 860 characteristics for the Tibet Plateau. The total sunshine hours in 2016 were from China  
 861 meteorological data sharing service system.



862



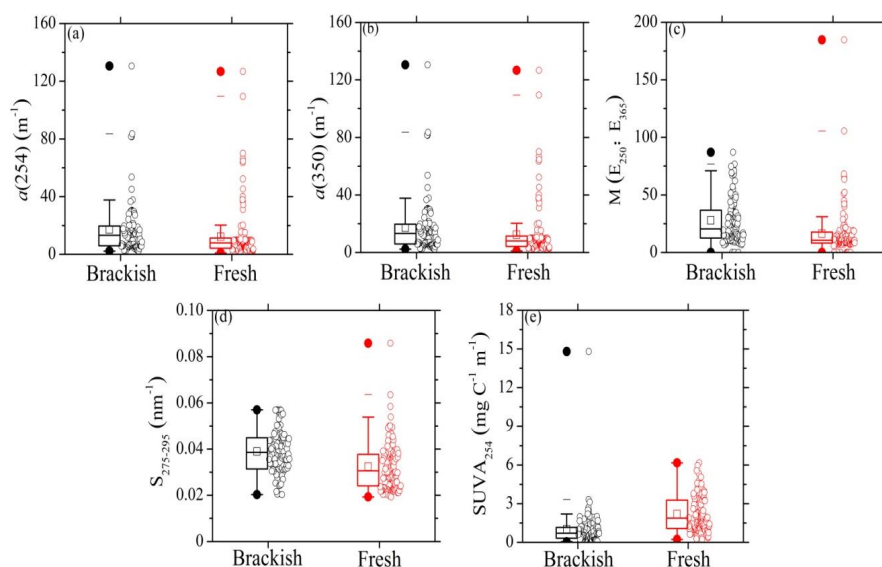
863 **Figure 2** The DOC, salinity and elevation from 63 lakes collected in Tibet Plateau, (a)  
864 The elevation (m) of 63 lakes in Tibet Plateau and corresponding DOC concentrations,  
865 and (b) Mean DOC and salinity (EC) of 63 lakes. The full line represents the tendency  
866 linear equation of average DOC concentrations. The numbers was the lake name  
867 according to Table S1.



868



**Figure 3.** Box plots of  $a(254)$  (a),  $a(350)$  (b),  $M(E_{250}: E_{365})$  (c),  $S_{275-295}$  (d) and  $SUVA_{254}$  (e) for brackish and fresh waters in the Tibet Plateau. The black line and the hollow squares represent the median and mean values, respectively. The horizontal edges of the boxes denote the 25th and 75th percentiles; the whiskers denote the 10th and 90th percentiles. The black circles represent samples of brackish lakes, and red were fresh lakes. Then the unit of  $SUVA_{254}$  is  $\text{mg C}^{-1} \text{m}^{-1}$ ,  $S_{275-295}$  is  $\text{nm}^{-1}$ , and CDOM absorption at 254 nm and 350 nm is  $\text{m}^{-1}$ .



876



**Figure 4.** Four typical EEM fluorescence spectra (a-d) and FRI results, (a) Lake DZC, (b) Lake BMC, (c) Lake BMLMC, (d) Lake NMC, (e) The proportion and cumulative volume proportion of EEMFRI-extracted average FDOM components from five regions in brackish lakes and fresh lakes in Tibet Plateau and (f) distributions of percentages of EEM-FRI extracted FDOM.

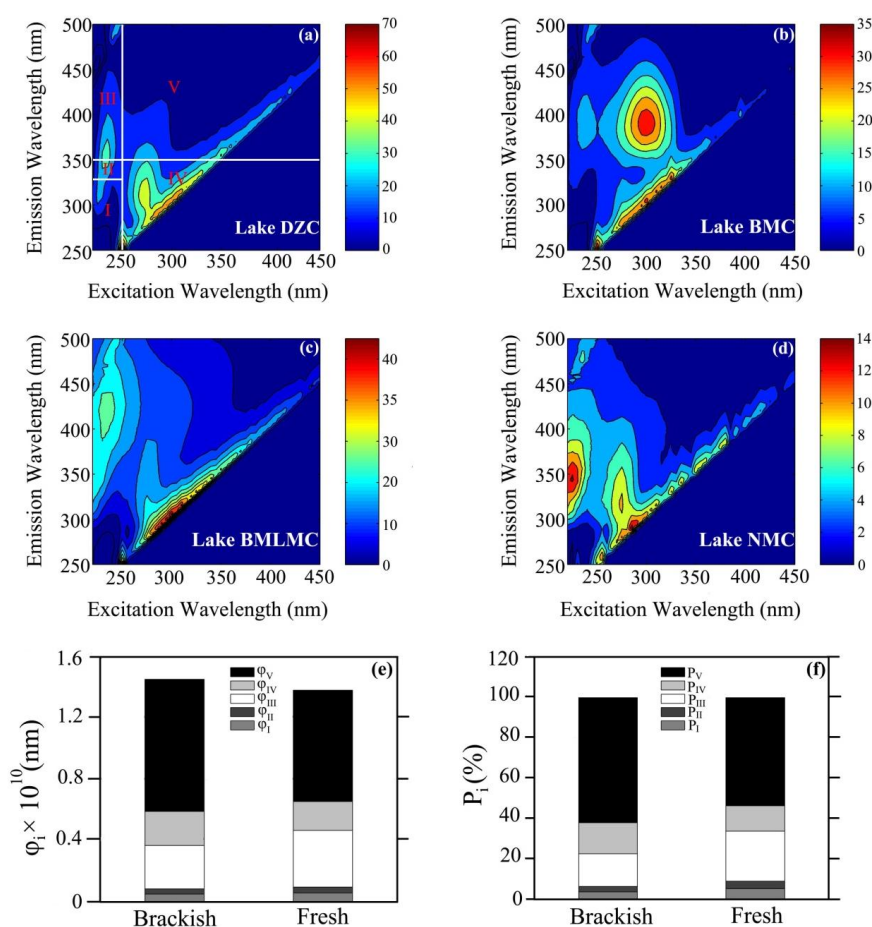
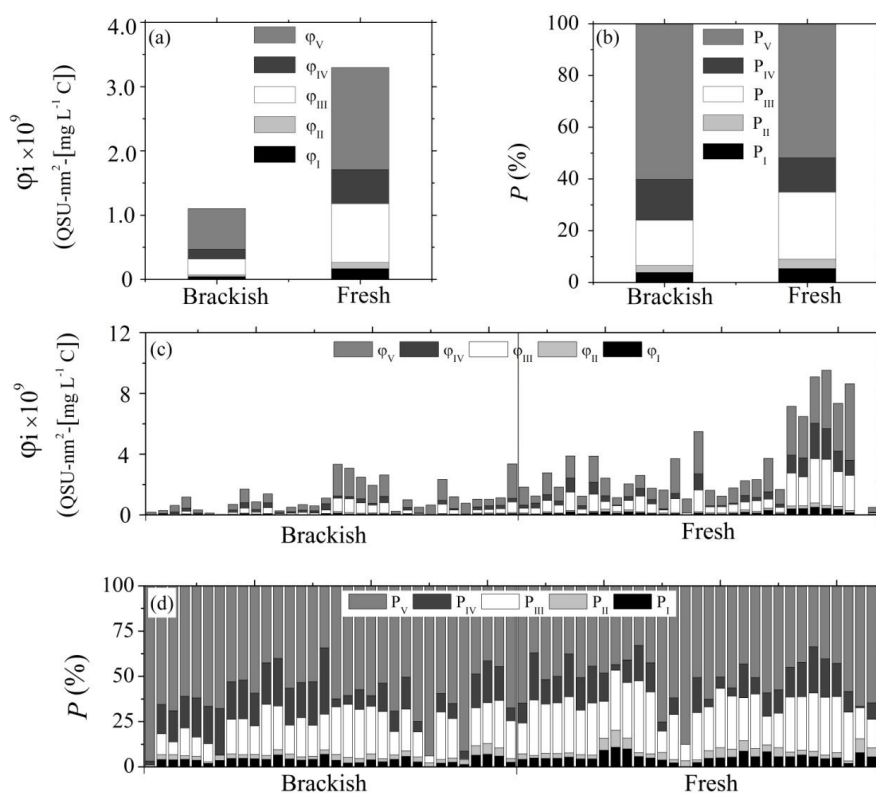




**Figure 5.** Normalized EEM-FRI fluorescence component and spatial characteristics from 63 lakes in Tibet Plateau, (a) normalized cumulative volume  $\phi_i$  of EEM-FRI extracted average FDOM components from five regions in brackish lakes and fresh lakes, (b) percentages  $P_i$  of EEM-FRI extracted FDOM in brackish lakes and fresh lakes, (c) spatial distributions of normalized cumulative volume  $\phi_i$  in brackish lakes and fresh lakes and (d) spatial distributions of percentages  $P_i$  of EEM-FRI extracted FDOM in brackish lakes and fresh lakes.



890



891 **Figure 6.** Box plots of  $HIX$  (a),  $FI_{370}$  (b) and  $FI_{310}$  (c) for brackish and fresh waters in  
892 the Tibet Plateau. The black line and the hollow squares represent the median and mean  
893 values, respectively. The horizontal edges of the boxes denote the 25th and 75th  
894 percentiles; the whiskers denote the 10th and 90th percentiles. The black circles  
895 represent samples of brackish lakes, and red were fresh lakes.

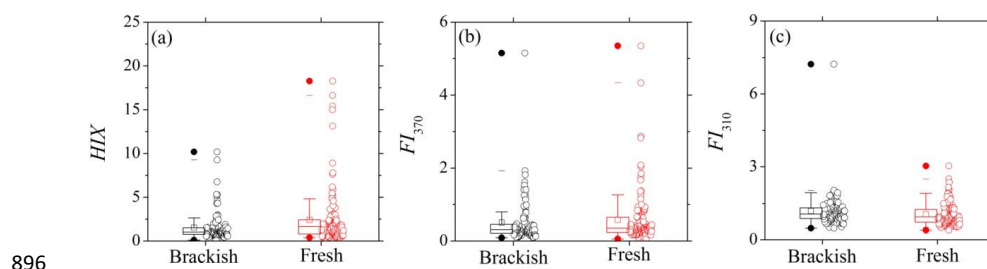




**Figure 7.** Principal component analysis (PCA) results of normalized cumulative volume  $\phi_i$  by EEM-FRI. (a) Loadings of PCA factors and (b) property-property plots of PCA factor scores of 63 lakes. The unit of normalized cumulative volume  $\phi_i$  ( $i=I, II, III, IV, V$ ) is  $QSU\text{-}nm^2\text{-}[mg\ L^{-1}\ C]$ .

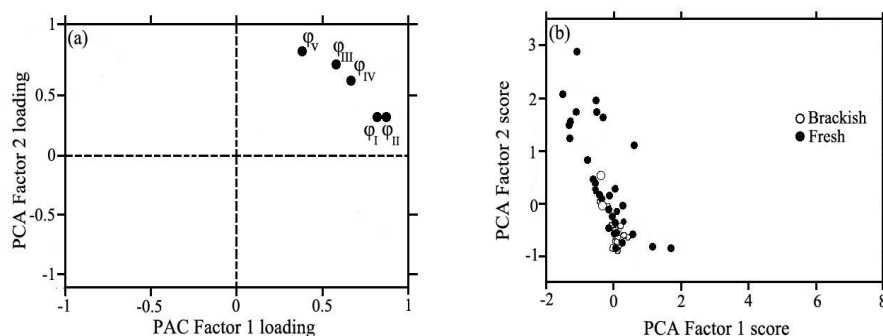
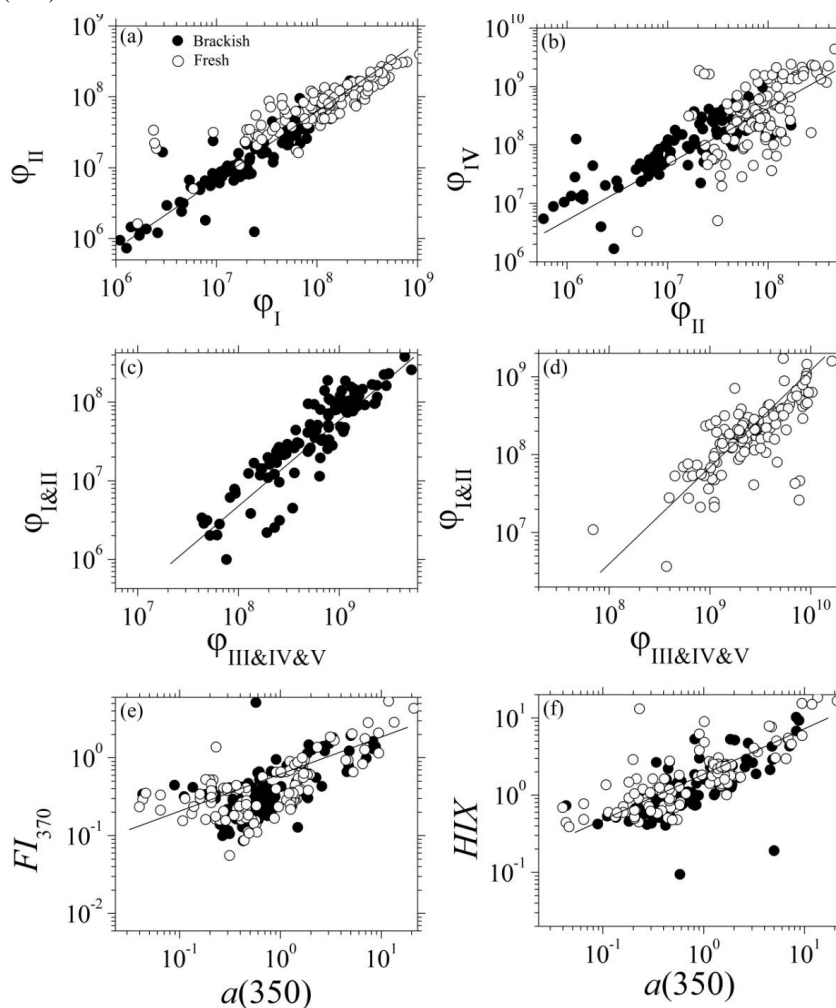




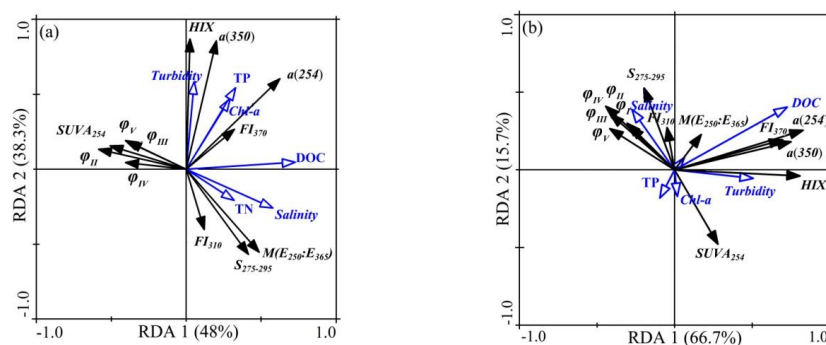
**Figure 8.** The correlations between normalized cumulative volume  $\phi_I$  and  $\phi_{II}$  by EEM-FRI for water samples in brackish lakes and fresh lakes (a); the correlations between normalized  $\phi_I$  and  $\phi_{IV}$  (b); the correlations between normalized  $\phi_{II}$  and  $\phi_{IV}$  (c); the correlations between normalized  $\phi_{III\&IV\&V}$  and  $\phi_{I\&II}$  by EEM-FRI (d); the correlations between  $a(350)$  and  $FI_{370}$  (e), and the correlations between  $a(350)$  and  $HIX$  (f). The unit of normalized cumulative volume  $\phi_i$  ( $i=I, II, III, IV, V$ ) is  $QSU\cdot nm^2\cdot [mg\ L^{-1}\ C]$ , and  $a(350)$  was  $nm^{-1}$ .



909

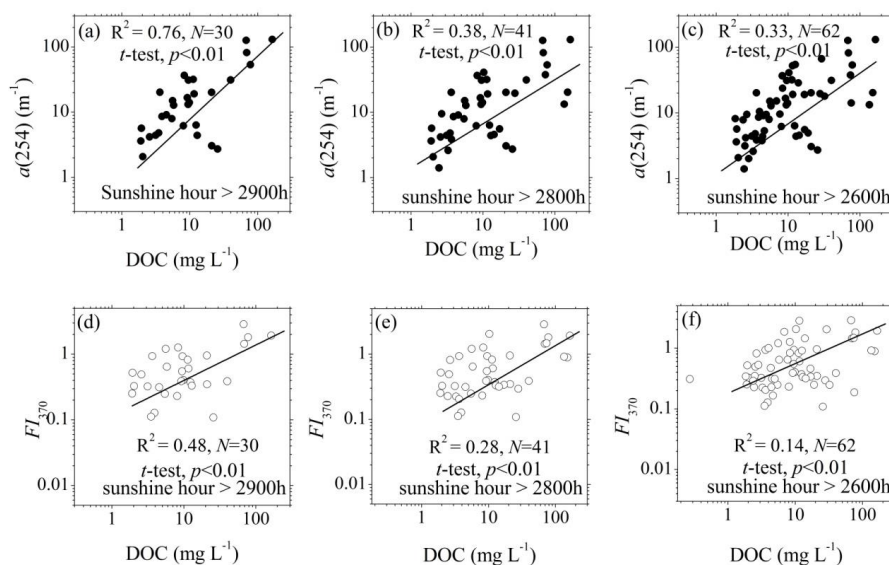


910 **Figure 9.** Redundancy analysis (RDA) of CDOM spectroscopic parameters and the  
 911 water quality parameters **(a)** brackish lakes and **(b)** fresh lakes **Tibetan Plateau**.  $\varphi_i$   
 912 was deleted due to large inflation factor ( $>20$ ). The solid arrows **and black font** represent  
 913 the environmental explanatory variables, and **hollow allows and blue fonts** were species  
 914 variables, respectively. **(c) and (d)** are the correlation between  $a(254)$ , DOC and  $FI_{370}$   
 915 in brackish and fresh lakes. The unit of TN, TP and DOC was  $\text{mg L}^{-1}$ ; Chl-a was  $\mu\text{g L}^{-1}$ ;  
 916  $a(254)$  and  $a(350)$  is  $\text{m}^{-1}$ ;  $SUVA_{254}$  is  $\text{L mg C}^{-1} \text{m}^{-1}$ ;  $\varphi_i$  ( $i=\text{I, II, III, IV, V}$ ) is  $\text{QSU-nm}^{-2}\cdot[\text{mg L}^{-1}$   
 917  $\text{C}]$ .





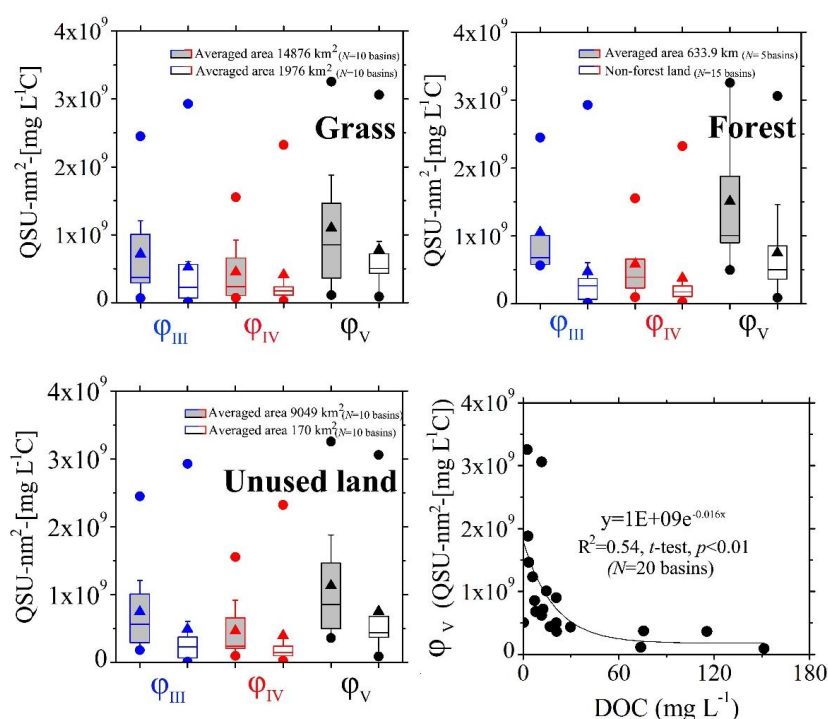
920 **Figure 10.** The correlation between average DOC concentrations and  $a(254)$  in annual  
 921 total sunshine hours > 2900h (a), annual total sunshine hours > 2800h (b) and annual  
 922 total sunshine hours > 2600h (c). Then the correlation between average DOC  
 923 concentrations and  $FI_{370}$  in annual total sunshine hours > 2900h (d), annual total  
 924 sunshine hours > 2800h (e) and annual total sunshine hours > 2600h (f). The annual  
 925 total sunshine hours in Tibet are from the China metrological data sharing service  
 926 system.



927



**Figure 11.** (a) Box plots of normalized  $\phi_{III}$ ,  $\phi_{IV}$  and  $\phi_V$  in basins with large grass area (averaged area 14876 km<sup>2</sup>;  $N=10$  basins, B1, B10, B19, B2, B11, B17, B12, B5, B20, B14), and basins with small grass area (averaged area 1976 km<sup>2</sup>;  $N=10$  basins, B4, B6, B8, B9, B3, B15, B18, B16, B13, B17). (b) Box plots of normalized  $\phi_{III}$ ,  $\phi_{IV}$  and  $\phi_V$  in basins with large forest area (averaged area 633.9 km<sup>2</sup>;  $N=5$  basins, B2, B1 B4, B11, B10), and in non-forest land. (c) Box plots of normalized  $\phi_{III}$ ,  $\phi_{IV}$  and  $\phi_V$  in basins with large unused land area (averaged area 9049 km<sup>2</sup>;  $N=10$  basins, B1, B4, B2, B17, B3, B10, B11, B20, B19, B12), and basins with small grass area (averaged area 170 km<sup>2</sup>;  $N=10$  basins, B6, B14, B8, B9, B15, B16, B7, B13, B5, B18). The black line and the hollow squares represent the median and mean values, respectively. The horizontal edges of the boxes denote the 25th and 75th percentiles; the whiskers denote the 10th and 90th percentiles. (d) The correlation between DOC and normalized humic like  $\phi_V$  of 20 basins in Tibet Plateau.





943 **Table 1** Water quality parameters of samples from 63 lakes ( $N=244$ ) in Tibet Plateau

Parameters	Brackish Lakes ( $N=109$ )		Fresh Lakes ( $N=135$ )	
	Mean	Max-Min	Mean	Max-Min
Turbidity	14.63±24.40	0-87.78	16.7±43.61	0-212.51
EC	8880.23±8235.912	1673-33141.2	536.55±332.29	120.1-1369.2
Salinity	6.01±5.60	1.14-22.54	0.36±0.22	0.08-0.93
TN	4.54±4.32	0.31-15.56	2.31±2.64	0.16-10.15
TP	0.45±1.35	0.006-6.79	0.04±0.03	0.001-0.08
Chl-a	2.57±5.73	0-31.37	1.4±2.68	0.09-14.68
DOC	35.69±43.52	0.27-164.8	7.94±12.17	1.84-67.79

944 TN, TP, DOC, DTC, and DIC represent total nitrogen, total phosphorus, dissolved organic carbon,  
 945 dissolved total carbon and dissolved inorganic carbon concentrations, respectively ( $\text{mg L}^{-1}$ ). EC  
 946 represents the electrical conductivity of water samples ( $\mu\text{S cm}^{-1}$ ). Chl-a, chlorophyll-a concentration  
 947 ( $\mu\text{g L}^{-1}$ ). The unit of turbidity is NTU, nephelometric turbidity unit, and salinity is ‰.



948 **Table 2** Regression analysis equations of DOC concentration and normalized cumulative volume  $\varphi_i$

949 ( $i$ =I, II, III, IV, V) for all the water samples from 63 lakes ( $N=244$ ) in Tibet Plateau

Salinity	Averaged EC	Regression equation	R <sup>2</sup>
<b>DOC &amp; <math>\varphi_I</math> (Tyrosine like)</b>			
>19	23764	$y=3E+07e^{-0.013x}$ , ( $N=29$ )	0.73
>7	10945	$y=3E+07e^{-0.014x}$ , ( $N=64$ )	0.42
>2	5708	$y=3E+07e^{-0.014x}$ , ( $N=84$ )	0.34
>1	2119	$y=4E+07e^{-0.015x}$ , ( $N=109$ )	0.34
<1	586	$y=1E+08e^{-0.034x}$ , ( $N=135$ )	0.03
<b>DOC &amp; <math>\varphi_{II}</math> (Tryptophan like)</b>			
>19	23764	$y=1E+07e^{-0.009x}$ , ( $N=29$ )	0.64
>7	10945	$y=2E+07e^{-0.012x}$ , ( $N=64$ )	0.41
>2	5708	$y=2E+07e^{-0.012x}$ , ( $N=84$ )	0.34
>1	2119	$y=2E+07e^{-0.014x}$ , ( $N=109$ )	0.34
<1	586	$y=8E+07e^{-0.023x}$ , ( $N=135$ )	0.03
<b>DOC &amp; <math>\varphi_{III}</math> (Fulvic like)</b>			
>19	23764	$y=9E+07e^{-0.009x}$ , ( $N=29$ )	0.30
>7	10945	$y=1E+08e^{-0.01x}$ , ( $N=64$ )	0.15
>2	5708	$y=2E+08e^{-0.01x}$ , ( $N=84$ )	0.08
>1	2119	$y=2E+08e^{-0.01x}$ , ( $N=109$ )	0.08
<1	586	$y=7E+08e^{-0.023x}$ , ( $N=135$ )	0.02
<b>DOC &amp; <math>\varphi_{IV}</math> (Microbial protein like)</b>			
>19	23764	$y=1E+08e^{-0.010x}$ , ( $N=29$ )	0.52
>7	10945	$y=1E+08e^{-0.012x}$ , ( $N=64$ )	0.37
>2	5708	$y=1E+08e^{-0.012x}$ , ( $N=84$ )	0.27
>1	2119	$y=1E+08e^{-0.012x}$ , ( $N=109$ )	0.28
<1	586	$y=4E+08e^{-0.034x}$ , ( $N=135$ )	0.02
<b>DOC &amp; <math>\varphi_V</math> (Humic like)</b>			
>19	23764	$y=4E+08e^{-0.008x}$ , ( $N=29$ )	0.59
>7	10945	$y=4E+08e^{-0.009x}$ , ( $N=64$ )	0.28
>2	5708	$y=4E+08e^{-0.009x}$ , ( $N=84$ )	0.23
>1	2119	$y=5E+08e^{-0.010x}$ , ( $N=109$ )	0.25
<1	586	$y=2E+09e^{-0.02x}$ , ( $N=135$ )	0.03
<b>DOC &amp; <math>\varphi_{III+VI+V}</math> (Humic like&amp; Microbial protein like &amp; Fulvic like)</b>			
>19	23764	$y=5E+08e^{-0.009x}$ , ( $N=29$ )	0.58
>7	10945	$y=6E+08e^{-0.01x}$ , ( $N=64$ )	0.30



>2	5708	$y = 7E+08e^{-0.01x}$ , ( $N=84$ )	0.24
>1	2119	$y = 8E+08e^{-0.011x}$ , ( $N=109$ )	0.26
<1	586	$y = 3E+09e^{-0.025x}$ , ( $N=135$ )	0.03

DOC &  $\phi_{I\&II}$  (Tyrosine like & Tryptophan like)

>19	23764	$y = 4E+07e^{-0.013x}$ , ( $N=29$ )	0.74
>7	10945	$y = 5E+07e^{-0.014x}$ , ( $N=64$ )	0.45
>2	5708	$y = 5E+07e^{-0.014x}$ , ( $N=84$ )	0.32
>1	2119	$y = 6E+07e^{-0.015x}$ , ( $N=109$ )	0.34
<1	586	$y = 2E+08e^{-0.03x}$ , ( $N=135$ )	0.03

950 The unit of EC is  $\mu\text{S cm}^{-1}$ ; salinity is ‰; DOC concentration is  $\text{mg L}^{-1}$ ;  $\phi_i$  ( $i=I, II, III, IV, V$ ) is QSU-  
 951  $\text{nm}^2\text{-[mg L}^{-1}\text{ C]}$ .